Structures and Properties of Multinuclear Copper Complexes Formed through Spontaneous Reactions and Self-Assembly

（自発的反応と自己集合により形成する多核銅錯体の構造と特性）

January, 2024

Materials Applied Chemistry　Major

Graduate School of Science and Technology

Doctoral Course

Nihon University

Yosuke Hosoya

Table of contents

Chapter 1

Introduction

1-1. Metal Complexes

A metal complex refers to a molecule where ligands are bound to a metal ion. These metal ions include a wide range of metals, such as p-block elements, transition metals, lanthanides, and actinides. Ligands are substances that form coordination bonds to metal ions, mainly organic molecules and inorganic ions. The coordination bond is formed when the ligand is placed around the metal ion. Metal complexes can exhibit diverse properties and functionalities based on the combination of the metal ion and ligands. Leveraging these varied properties, extensive research is conducted, ranging from applications as catalysts utilizing metal ions as active sites to the development of chromic molecules or molecular magnetic materials that utilize complex interactions between intricate molecules (Fig. 1.1).

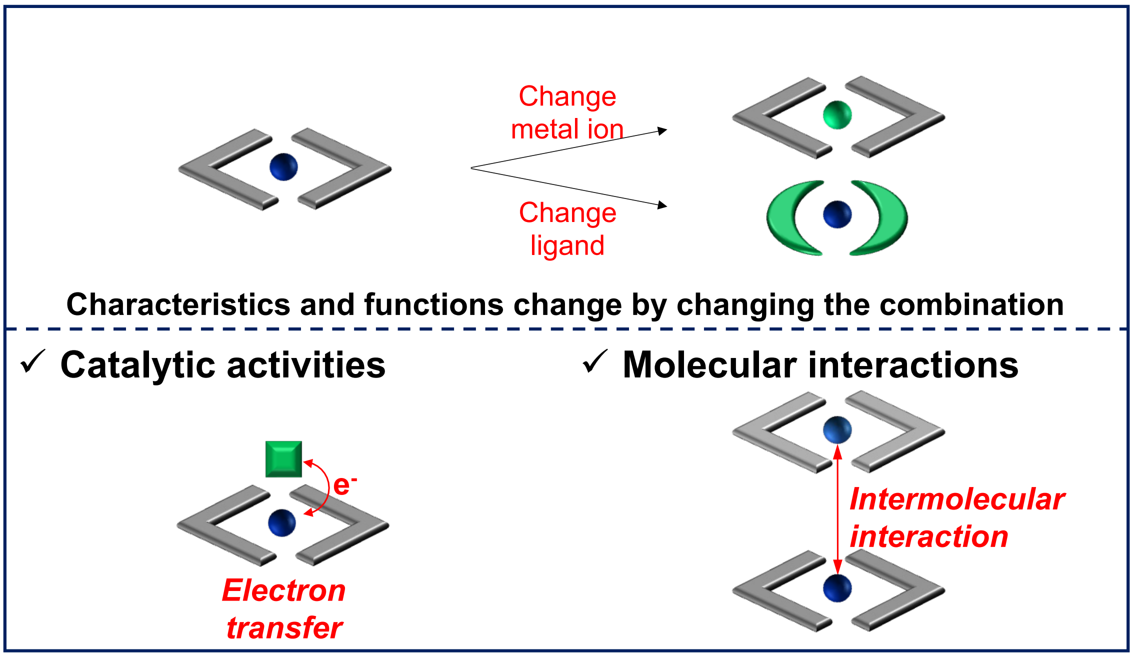

Fig. 1.1. Properties and functions of metal complexes.

1-2. Multinuclear Metal Complexes

Multinuclear metal complexes are complexes that contain multiple metal ions within a single molecule. Consequently, these complexes exhibit not only interactions between different complexes but also interactions between metals within a molecule mediated by ligands (Fig. 1.2). These complexes demonstrate unique properties and functions distinct from mononuclear complexes, attracting attention for various applications such as catalysts and molecular magnetic materials. Additionally, studies on multinuclear metal complexes containing internal spaces have been reported, which are widely explored in the research field of host molecules.

When multinuclear metal complexes function as catalysts, their mechanisms can be categorized into two types: where the metal ions within the molecule act as catalytic sites, or where the multinuclear metal complex functions as a microreactor. The cases introduced in Chapter 1-2-1 involve instances of the former, while Chapter 1-2-2 represents cases of the latter. These characteristics can be flexibly altered by designing ligands and combinations with metal ions. Multinuclear metal complexes offer the ability to control the distance between metal ions through ligand selection. This capability enables more efficient catalyst design compared to mononuclear complexes, primarily studied for applications in organic synthesis.[1-4]

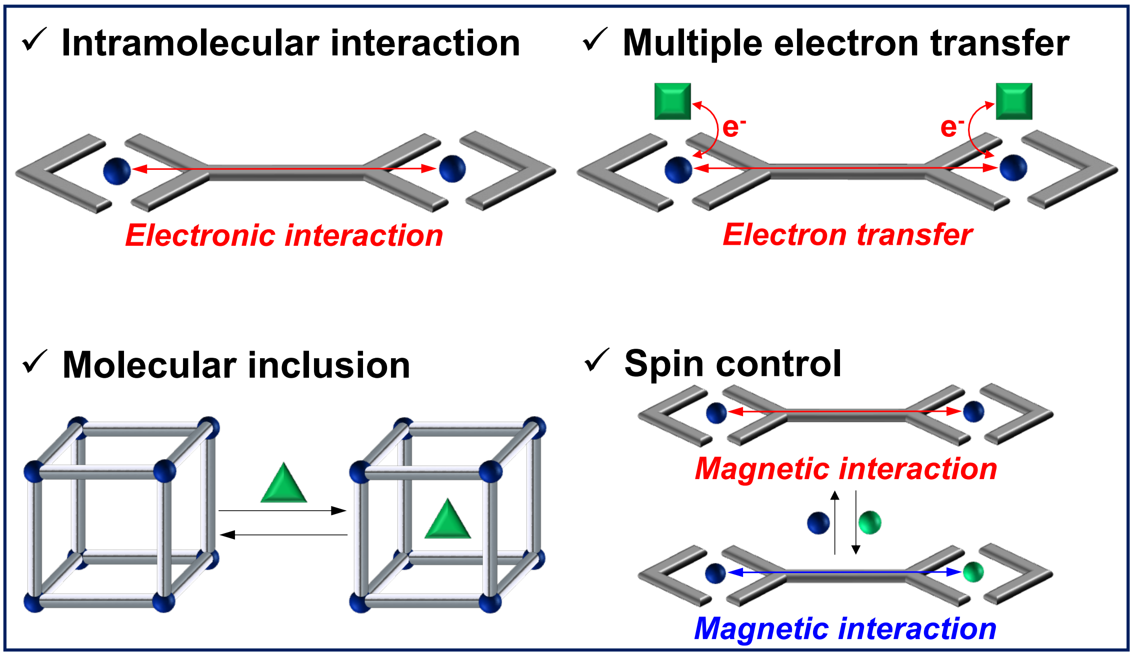

Fig. 1.2. Properties and functions of multinuclear metal complexes.

1-2-1. Research on Catalysts Using Multinuclear Metal Complexes

A. Arbaoui et al. discovered that a binuclear aluminum complex **1** exhibited higher activity than a mononuclear complex in the ring-opening polymerization of caprolactone (Fig. 1.3a).[1] In complex **1**, one aluminum ion coordinated with the monomer while the other coordinated with the initiator, allowing the initiator to efficiently attack the monomer, resulting in this difference in activity.

P. K. Saini et al. synthesized a hetero-binuclear complex **2**, showing high activity in the copolymerization of cyclohexene and carbon dioxide (Fig. 1.3b).[2] This complex **2** exhibited higher catalytic activity compared to binuclear zinc and magnesium complexes with the same structure.

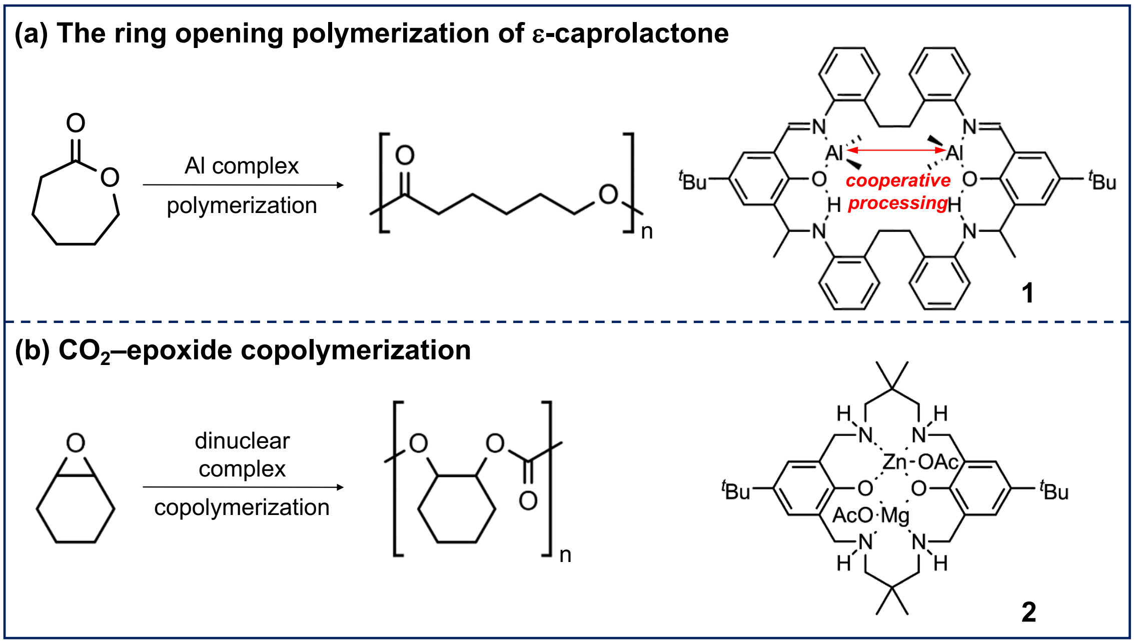

Fig. 1.3. Multinuclear metal complexes that function as catalysts for organic synthesis.

In addition to their use in organic synthesis, multinuclear metal complexes have been extensively investigated for their catalytic applications in water redox and carbon dioxide reduction (Fig. 1.4).[5-8]

K. Yamauchi et al. discovered that a dinuclear platinum complex **3** acts as an effective catalyst for water reduction (Fig. 1.4a).[6] The electronic interaction between the two platinum ions within the molecule destabilizes the highest-occupied molecular orbital (HOMO) of the complex, enhancing its hydrogen-producing ability compared to mononuclear platinum complexes.

M. Okamura et al. reported that a pentanuclear iron complex **4** functions as a highly efficient oxygen-evolving catalyst (Fig. 1.4b).[8] This complex can efficiently form an O-O bond by coordinating two water molecules to the two iron ions within the molecule. Consequently, it exhibited a higher oxygen generation efficiency compared to the mononuclear iron complex.

O. Ishitani et al. found that a heterodinuclear Ru–Re complex **5** acts as a highly efficient carbon dioxide reduction catalyst (Fig. 1.4c).[5, 7] This complex, which is formed by combining a ruthenium complex functioning as a photosensitizer and a rhenium complex acting as a catalyst, undergoes efficient electron transfer within its structure. Therefore, complex **5** can reduce carbon dioxide more efficiently than when the ruthenium and rhenium complexes are used separately.

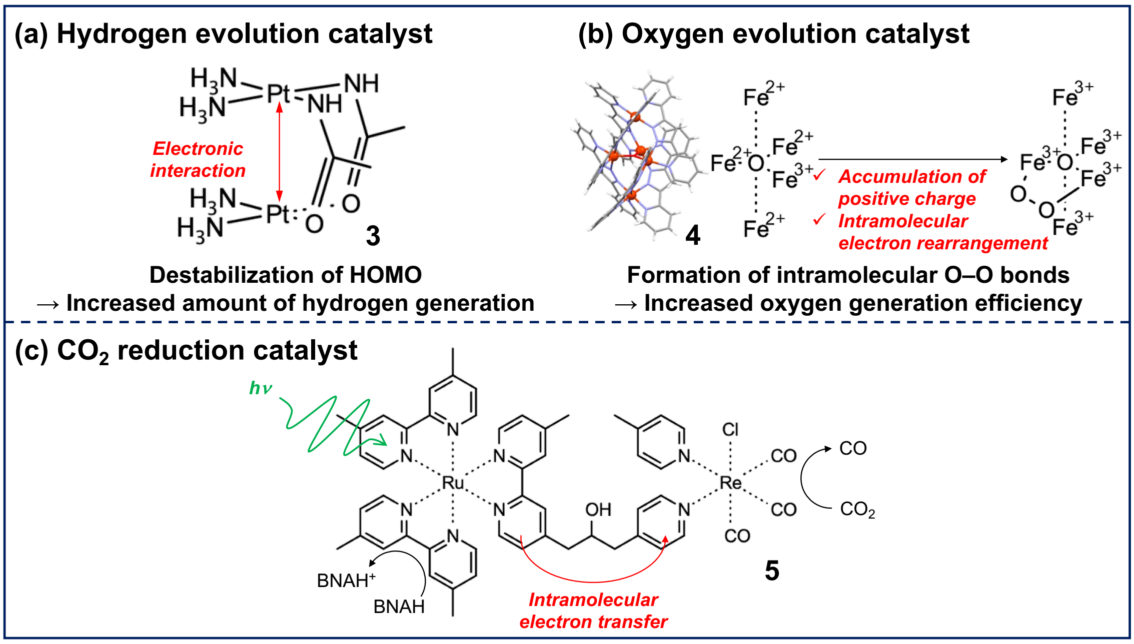

Fig. 1.4. Multinuclear metal complexes that function as water redox catalysts or catalysts for the reduction of carbon dioxide.

1-2-2. Studies Utilizing Multinuclear Metal Complexes as Host Molecules

Among multinuclear metal complexes, molecules with small spaces have been reported to function as host molecules. M. Yoshizawa et al. have created microenvironments using multinuclear metal complexes as host molecules to control reactions, such as the Diels-Alder reaction (Fig. 1.5).[9] A typical Diels-Alder reaction involving anthracene usually involves the 9,10-position of the anthracene. In the depicted reaction in Fig. 1.5b, compound **3** is synthesized. However, when employing a hexanuclear palladium complex **6** as a host molecule, an unexpected reaction occurs at the 1,4-position of the anthracene. Within the host molecule, these positions are situated in proximity to the dienophile (Fig. 1.5c), resulting in an atypical Diels-Alder reaction and the formation of compound **4**.

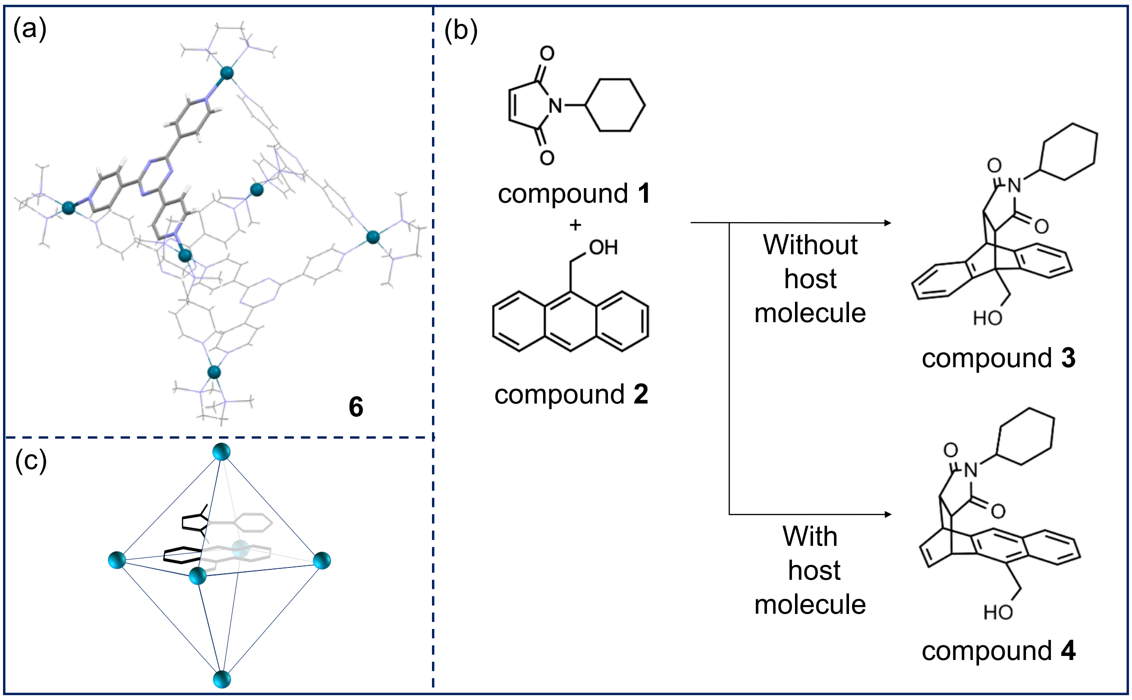

Fig. 1.5. The utilization of a hexanuclear palladium complex **6** as a host molecule. (a) Crystal structure. (b) Products of the Diels-Alder reaction depending on the presence or absence of the host molecule. (c) Disposition of compounds **1** and **2** within the host molecular structure.

1-2-3. Research on Molecular Magnetic Materials Utilizing Multinuclear Metal Complexes

Magnetism is the magnetic property determined by electrons within a substance. Every electron possesses a minute magnetic moment associated with its quantum mechanical 'spin.' The electrons exist within orbitals around atoms, and each orbital may contain two electrons. One is 'spin-up,' aligning its spin in the same direction as the external magnetic field, while the other is 'spin-down,' aligning its spin in the opposite direction to the external magnetic field. As a result, when spins cancel each other out, the substance shows diamagnetic behavior as a whole. Conversely, when there is an unpaired electron in an orbital, the substance exhibits paramagnetic behavior as a whole. The proximity of unpaired electrons to each other eventually affects the arrangement of adjacent spins. If this alignment leads to spins pointing in opposite directions, it results in antiferromagnetic behavior. In contrast, when spins in a solid align in the same direction, it demonstrates ferromagnetic behavior. Ferrimagnetism occurs when spins with different magnetic moments exist on adjacent sites, aligning antiferromagnetically without canceling each other out.[10]

Exposure of a substance to an external magnetic field, H, induces magnetization, M. For paramagnetic materials, M is proportional to H (eq 1.1).

$$M = \chi_{\mathrm{m}} H \qquad (1.1)$$

The proportionality constant χ_{m} is referred to as the molar magnetic susceptibility and its temperature dependence is characterized by the Curie expression (eq 1.2). This formula applies when the spins do not interact with each other and there is a single spin quantum number involved.

$$\chi_{\mathrm{m}} = \frac{C}{T} \qquad (1.2)$$

Here, T is the temperature. C is the Curie constant defined by the following equation (eq 1.3).

$$C = \frac{N_{\mathrm{A}}\mu_0\mu_{\mathrm{B}}^2 g^2 S(S+1)}{3k_{\mathrm{B}}} \qquad (1.3)$$

S represents the spin quantum number, N_{A} is Avogadro's constant, μ_0 is the magnetic permeability of vacuum, μ_{B} is the Bohr magneton, g is the Lande g-factor, and k_{B} is the Boltzmann constant. When multiple spin quantum numbers are involved, the Van Vleck equation (eq 1.4) applies.

$$\chi_{\mathrm{m}} T = \frac{N_{\mathrm{A}}\mu_0{\mu_{\mathrm{B}}}^2 g^2}{3k_{\mathrm{B}}} \frac{\Sigma_S\left[S(S+1)(2S+1)\exp\left(-\frac{E_S}{k_{\mathrm{B}}T}\right)\right]}{\Sigma_S\left[(2S+1)\exp\left(-\frac{E_S}{k_{\mathrm{B}}T}\right)\right]} \qquad (1.4)$$

Here, E_S is energy of the $2S+1$ multiplet. The magnetic behavior is explained by the Heisenberg model. In this model, spins are localized at paramagnetic centers, and the magnetic exchange interaction is assumed to be isotropic. The spin exchange operator is represented by eq 1.5.

$$\hat{H} = -2\sum J_{ij}\,\hat{\mathbf{s}}_i \cdot \hat{\mathbf{s}}_j \qquad (1.5)$$

$\hat{\mathbf{s}}_i$ and $\hat{\mathbf{s}}_j$ represent the spin operators representing the metal ions i and j, respectively, while J_{ij} indicates the exchange constant. In the case of antiferromagnetic interaction, J_{ij} is negative, whereas in ferromagnetic interaction, J_{ij} is positive.

Molecular magnetic materials that function at the molecular level have attracted attention since they can be designed flexibly and their magnetic properties can be precisely controlled compared to bulk magnetic materials. Metal complexes are extensively researched due to their magnetic properties absent in organic molecules. Particularly, polynuclear metal complexes exhibit unique characteristics arising from magnetic interactions among metal ions within the molecule, not observed in mononuclear metal complexes. Hence, their applications in studies related to single-molecule magnets (SMMs),[11] spin crossover (SOC) materials,[12] and single-chain magnets (SCMs)[13] are being explored. Research is being conducted to modify the magnetic properties by changing metal ions within the same ligands or by altering bridging ligands between identical complexes. (Fig. 1.6). Changing the metal ion is intended to significantly alter the magnetic properties of the substance as a whole,[14-16] while altering bridging ligands is performed to manipulate the intermolecular magnetic interactions.[17-21] There are fewer reported cases concerning the control of magnetic interactions through ligand modifications compared to studies involving the alteration of metal ions. In one instance, multinuclear metal complexes are interconnected using azide to create a one-dimensional chain. This results in magnetic properties distinct from those of a complex with a similar structure but in non-bridged configurations.[17, 19, 20] In another example, the molecular arrangement and magnetic susceptibility are altered by recrystallizing preformed crystals from solutions containing additional ligands.[18]

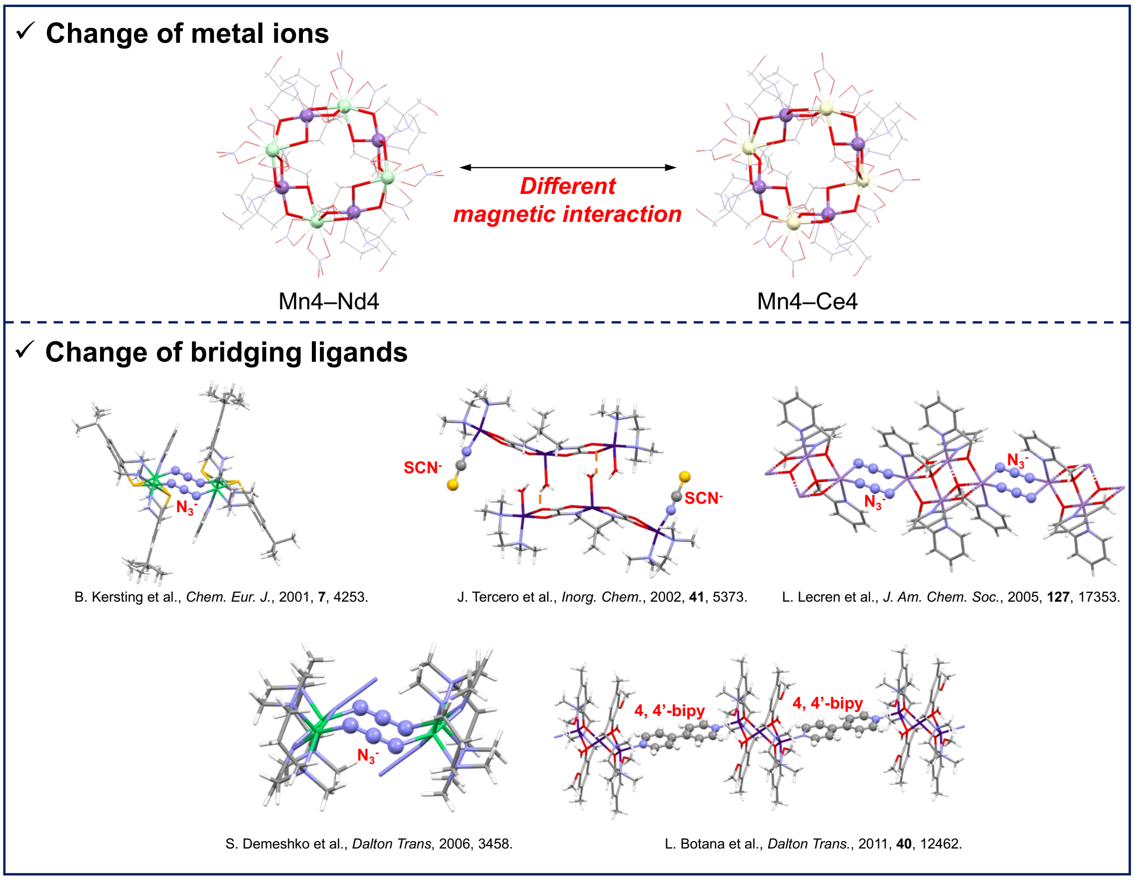

Fig. 1.6. Alterations in magnetic properties of polynuclear metal complexes.

1-3. Spontaneous Reactions and Self-Assemblies During Complex Formation

Many multinuclear metal complexes have been synthesized in the past. In these studies, complexes with desired physical properties and characteristics are synthesized by mixing pre-designed ligands and metal salts, facilitating their self-assembly. Conversely, some reports describe "spontaneous reactions" occurring during the complex formation, in which ligands undergo chemical changes, ultimately leading to the formation of complexes through the self-assembly of the altered ligands and metal ions (Fig. 1.7). The examples reported so far have used nitrile or 2,4-pentandione dioxime (AADO) as ligands.

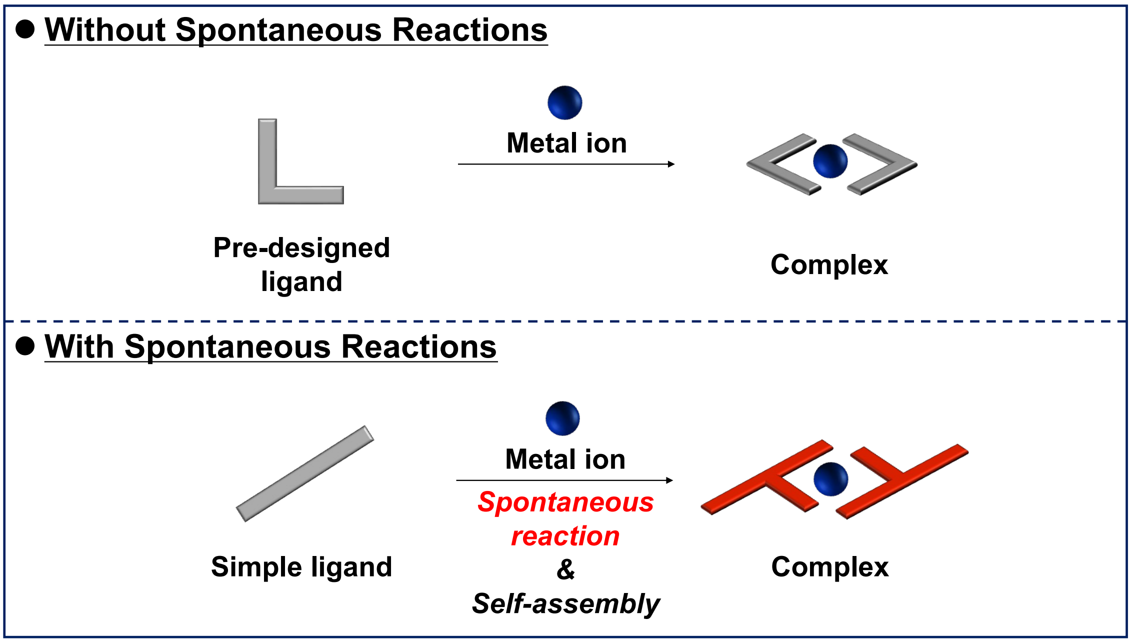

Fig. 1.7. Differences in complex formation based on the presence or absence of spontaneous reactions.

1-3-1. The Spontaneous Reactions and Self-Assembly That Occur During Complex Formation Using Nitrile

Several reports have indicated that when nitriles such as dicyanamide[22-24] or 2-pyrimidinecarbonitrile[25, 26] are employed as ligands along with copper(II) salt or cobalt(II) salt as metal salts, the terminal cyano group undergoes changes, resulting in the formation of mononuclear or multinuclear complexes through interactions with the metal ions.

When sodium dicyanamide and copper(II) ions are mixed in methanol, a reaction between the cyano group and methanol yields an amine with a methoxy group attached at the terminal.[22-24] L. L. Zheng et al. reported systems where the concentration of sodium dicyanamide in the reaction can be adjusted to allow attachment of methoxy groups to either one or both sides of the two cyano groups of dicyanamide (dca) (Fig. 1.8a).[23] In reaction systems with high concentrations of dca, a structural change occurs in the ligand, resulting in the methoxy group binding only to one side of the cyano group. They demonstrated that in systems with high dca concentrations, upon mixing copper(II) ions and nicotinamide, two nicotinamides and two unreacted dca coordinate with copper(II) ions, forming mononuclear copper complex **7** (Fig. 1.8b). In the crystal, copper(II) ions are bridged by the unreacted two dca, forming one-dimensional chains. Furthermore, hydrogen bonding occurs between the methoxy-attached dca and nicotinamide, resulting in the formation of additional one-dimensional chains distinct from the previously mentioned chains (Fig. 1.8c). In a reaction with low dca concentration, the ligand undergoes a structural change wherein methoxy groups are bonded to both sides of the cyano groups in dca. When $Cu(ClO_4)_2$ as the copper(II) salt was mixed with sodium dicyanamide, a mononuclear copper complex **8** was formed.[23] In the crystals, hydrogen bonds formed between the NH hydrogen not coordinated to the copper ions and water molecules (Fig. 1.8d). Further hydrogen bonding between water molecules and perchlorate ions results in the formation of a one-dimensional chain.

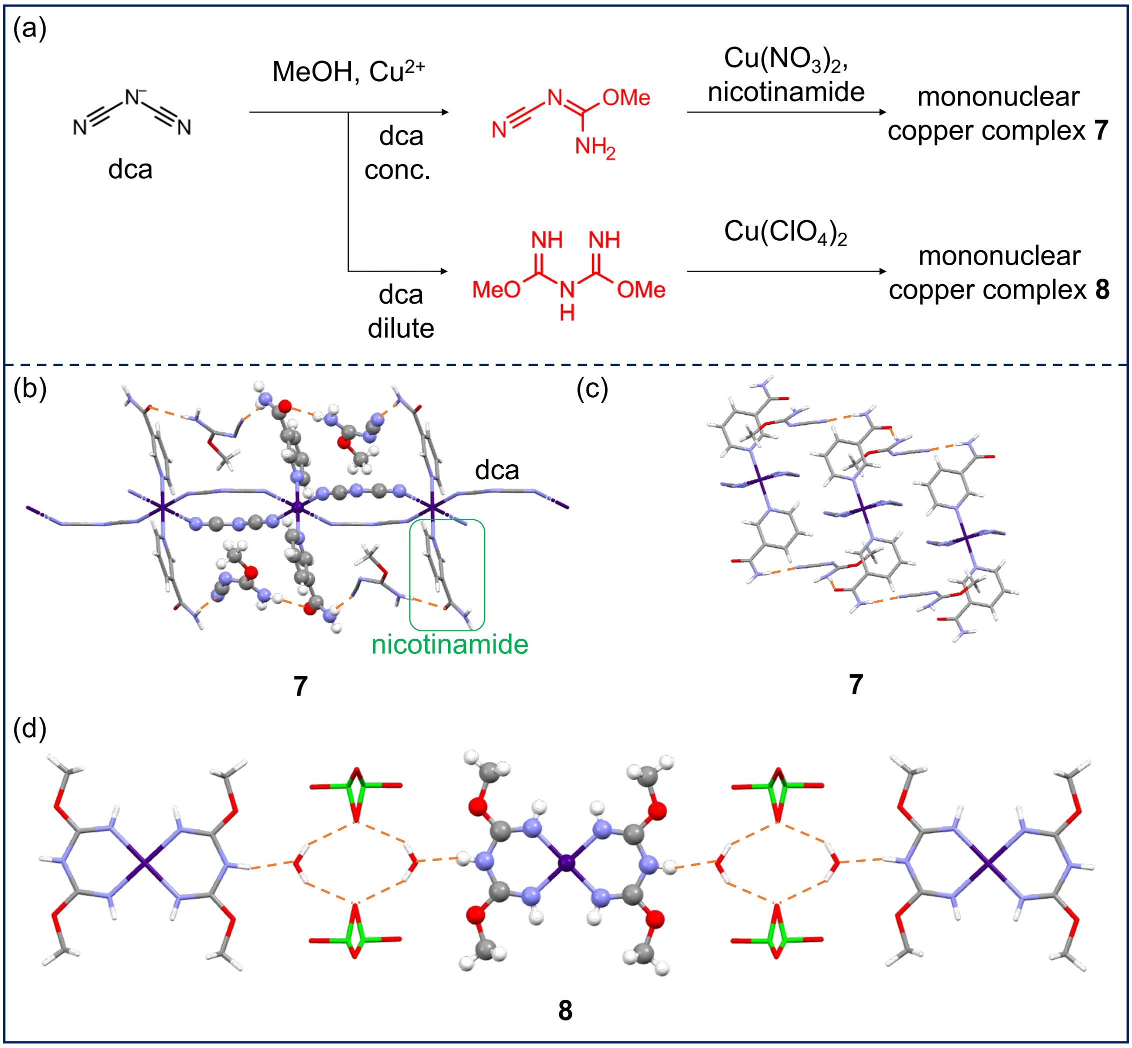

Fig. 1.8. Spontaneous reactions and self-assembly of nitrile in the presence of copper ions (H, white; C, gray; N, blue; O, red; Cl, green; Cu, purple). (a) Reaction formulae. Complex **7**: (b) view from the *a*-axis direction, (c) view from the *b*-axis direction. Complex **8**: (d) view from the *b*-axis direction.

D. B. Eni et al. observed the introduction of methoxy groups from solvent methanol to both cyano groups of dca during the formation of copper complexes when dca, copper(II) ions, and 1,10-phenanthroline were mixed (Fig. 1.9a).[24] In this system, a mononuclear copper complex **9** is formed by the coordination of one modified ligand and one 1,10-phenanthroline ligand to the copper(II) ion (Fig. 1.9b). Upon changing the metal salt to cobalt(II) salt, dca no longer reacts with the solvent methanol but instead reacts among themselves to form dicyanoguanidinate. In this system, two 1,10-phenanthroline ligands coordinate to the cobalt(II) ion, forming a mononuclear cobalt complex **10**. While the dicyanoguanidinate generated by the structural transformation of dca itself does not form a coordination bond with the cobalt ion, it exists in the crystal as the counter-anion of the cobalt complex along with the nitrate ion (Fig. 1.9c).[24]

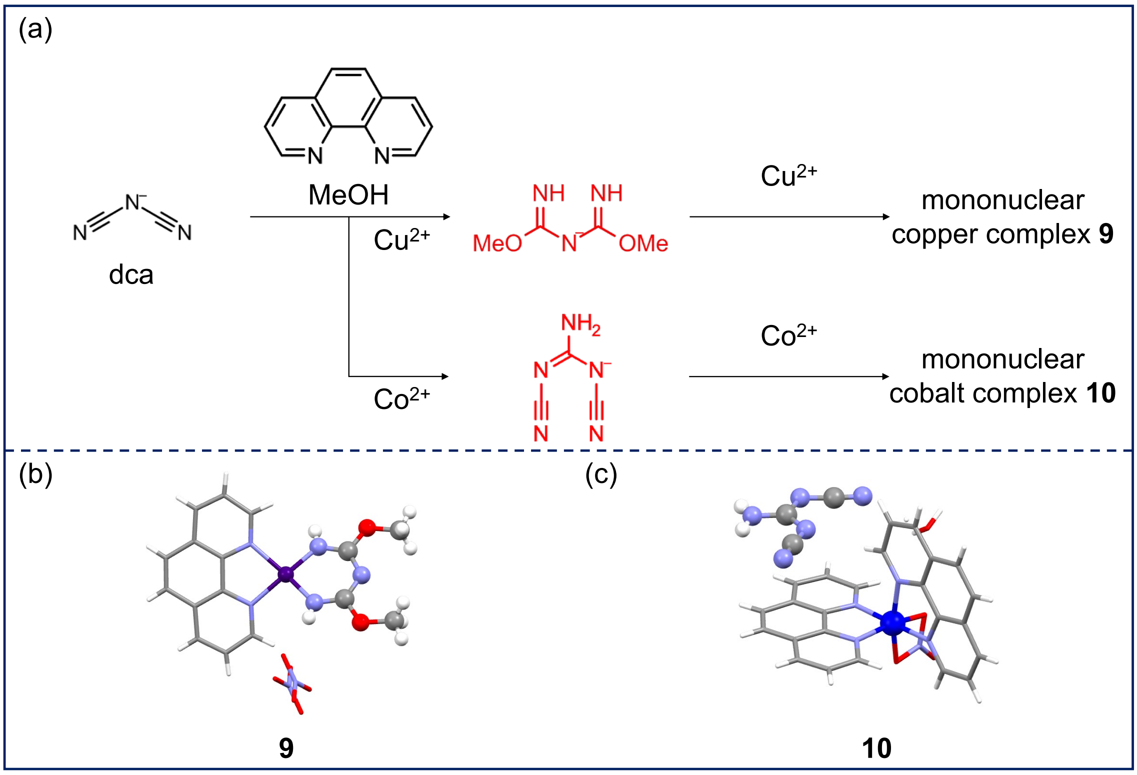

Fig. 1.9. Complexation of dicyanamide with metal ions in the presence of 1,10-phenanthroline (H, white; C, gray; N, blue; O, red; Co, blue; Cu, purple). (a) Reaction formulae. (b) Crystal structure for complex **9**. (c) Crystal structure for complex **10**.

In systems like those in Fig. 1.8 and 1.9, only mononuclear metal complexes are obtained. However, when pyrazole is added to a system containing nitrile and metal salts, either mononuclear or multinuclear metal complexes are formed. In these systems, the nitrile reacts with pyrazole, leading to the formation of complexes through the resulting modified ligands and metal ions. L. L. Zheng et al. successfully produced both mononuclear and trinuclear copper complexes by adjusting the amount of pyrazole (Fig. 1.10a).[23] When the amount of pyrazole in the reaction system is half that of dca, some of the dca reacts with pyrazole, while the remaining unreacted dca reacts with the solvent methanol. The dca reacting with pyrazole binds pyrazole to only one of the two cyano groups, leaving the other side unreacted. Dca reacting with methanol attaches methoxy groups to both cyano groups. Coordination of both of these modified ligands to the copper(II) ion results in the formation of a mononuclear copper complex **11**. In the crystal structure, hydrogen bonds are observed between the unreacted portions of dca within the copper complex and the imino groups of ligands in the adjacent copper complex (Fig. 1.10b). When a mixed solution containing sodium dicyanamide and pyrazole in a 1:3 ratio is introduced to $Cu(ClO_4)_2$, followed by the addition of $AgNO_3$, both cyano groups of dca react with pyrazole and self-assemble with copper(II) ions, resulting in the formation of trinuclear copper complex **12** (Fig. 1.10c). In the reaction system leading to the formation of complex **13** (Fig. 1.10d), involving sodium dicyanamide and pyrazole in a 2:1 ratio and using $AgBF_4$ as the silver salt, both cyano groups of dca react with pyrazole, akin to the reaction seen in complex **12**.[23]

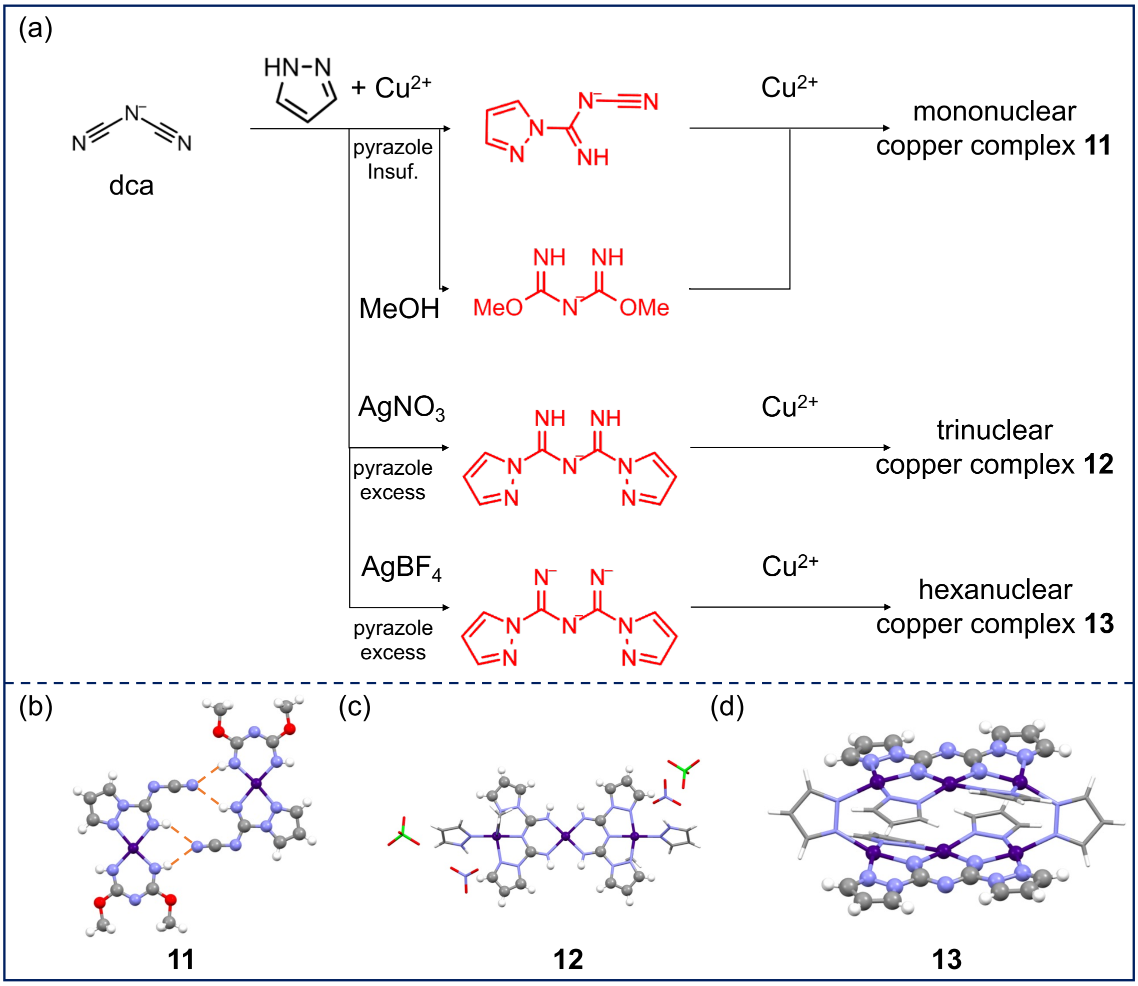

Fig. 1.10. The chemical transformation of pyrazole and dicyanamide and their complex formation with copper(II) ions (H, white; C, gray; N, blue; O, red; Cl, green; Cu, purple). (a) Reaction formulae. (b) Crystal structure of complex **11**. (c) Crystal structure of complex **12**. (d) Crystal structure of complex **13**.

L. L. Zheng et al. discovered in 2020 that by further changing the type of nitrile, mononuclear and tetranuclear copper complexes can be obtained through spontaneous reactions and self-assembly (Fig. 1.11a).[25] Using the simplest nitrile, acetonitrile, along with copper(II) ions and pyrazole, they observed the reaction between the cyano group of acetonitrile and pyrazole. This led to the formation of a mononuclear copper complex **14** with two structurally modified ligands. In the crystal, this complex showed hydrogen bonding between water molecules coordinated to copper ions and nitrate ions, and further hydrogen bonding occurred between the nitrate ions and the imino groups of the ligands within the copper complex, forming a one-dimensional chain (Fig. 1.11b). Similarly, when 2-pyrimidinecarbonitrile was used as the nitrile, the reaction between the cyano group and pyrazole resulted in the formation of a copper complex **15**. In this complex, a tetranuclear copper complex forms through the coordination of two structurally modified ligands and four pyrazoles to four copper(II) ions. Furthermore, the coordination of methanol and perchlorate ions to the copper(II) ion creates a one-dimensional chain (Fig. 1.11c).[4]

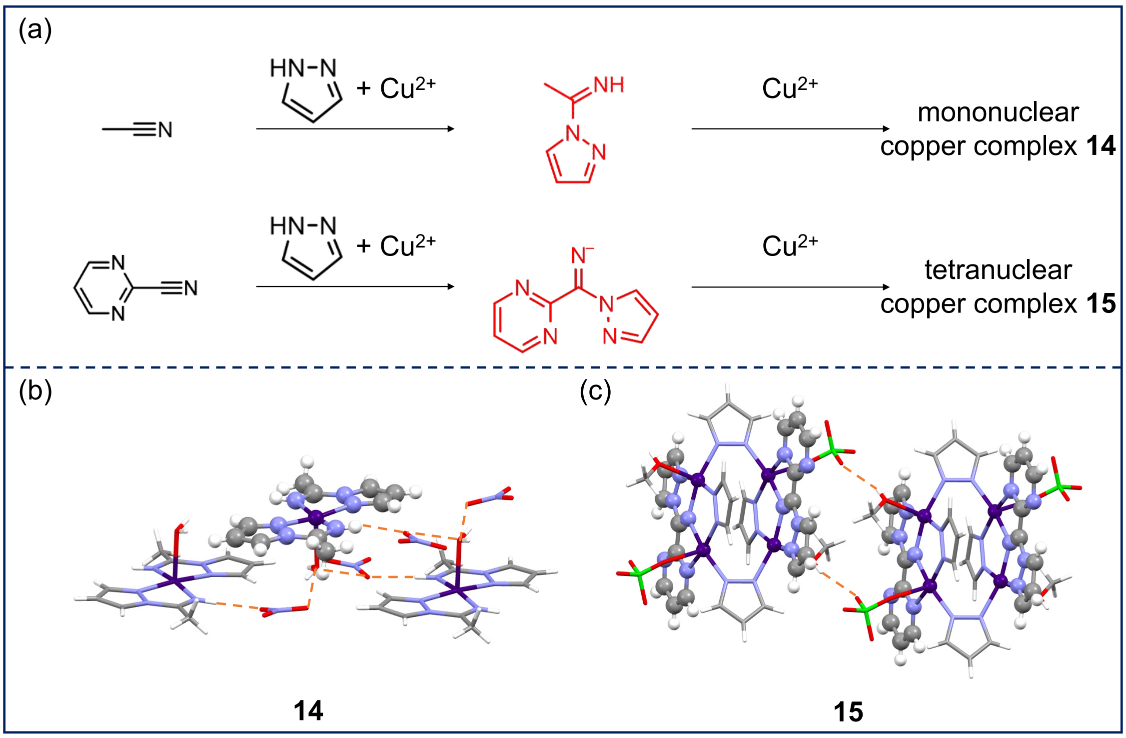

Fig. 1.11. Structural modifications of nitriles in the presence of pyrazole and copper(II) ions, leading to the formation of copper complexes (H, white; C, gray; N, blue; O, red; Cl, green; Cu, purple). (a) Reaction formulae. (b) Crystal structure of complex **14**. (c) Crystal structure of complex **15**.

Additionally, in 2022, they described the formation of a tetranuclear heterometallic complex **16** using two different metal salts, copper(II) salt and cobalt(II) salt, under a nearly identical reaction conditions (Fig. 1.12a).[26] Similar to complex **15** they reported in 2020, this system utilized twice the amount of pyrazole compared to 2-pyrimidinecarbonitrile during complex formation. However, the 2-pyrimidinecarbonitrile underwent two types of structural modifications during the complex formation process. One type involved the reaction of the cyano group with pyrazole, while the other involved a reaction with the solvent methanol, resulting in the introduction of methoxy groups as ligands. Of the two structurally modified ligands, only the one reacted with pyrazole possesses deprotonated imino groups, leading to a charge of -1. Complex **16** is formed by the coordination of two types of modified ligands and four deprotonated pyrazoles to two copper(II) and two cobalt(III) ions (Fig. 1.12b).

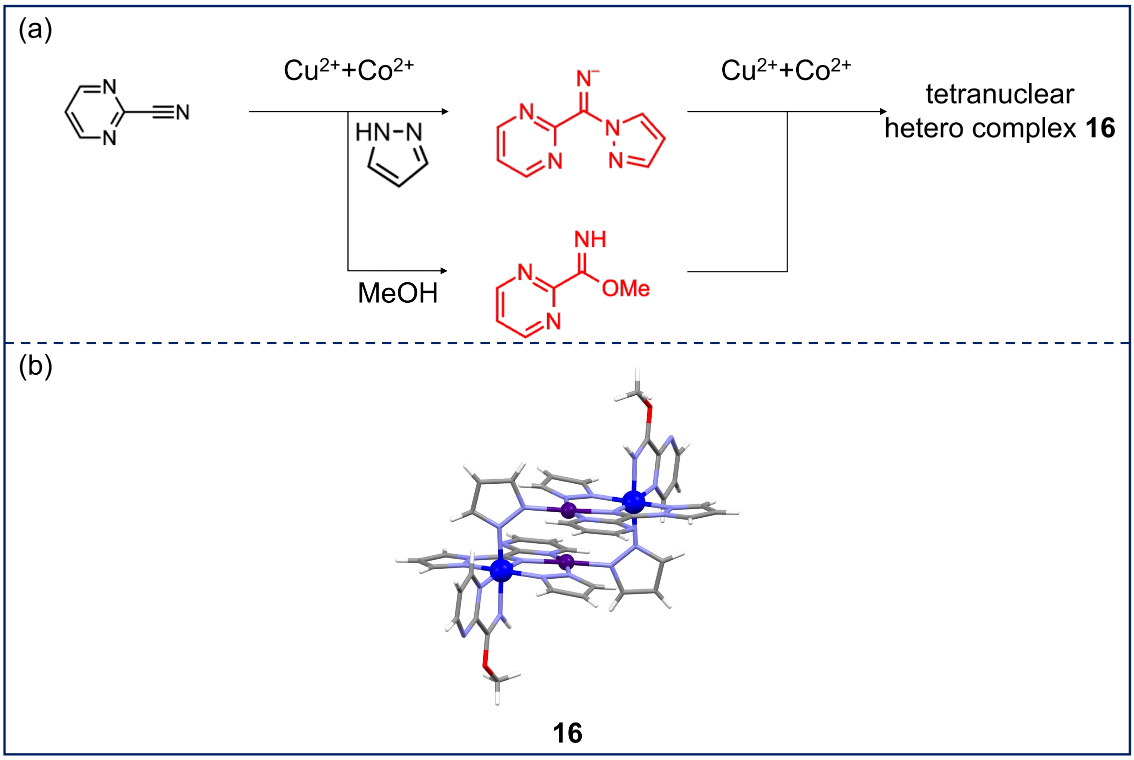

Fig. 1.12. The structural transformation and complex formation of pyrazole and 2-pyrimidinecarbonitrile in the presence of copper(II) and cobalt(II) ions (H, white; C, gray; N, blue; O, red; Cu, purple ball; Co, blue ball). (a) Reaction formulae. (b) Crystal structure of complex **16**. Purple ball: copper(II), blue ball: cobalt(II). The solvent molecules and perchlorate ions present in the crystals are omitted.

1-3-2. The Spontaneous Reactions and Self-Assembly That Occur During Complex Formation Using AADO

A few reports have indicated that when AADO is employed as a ligand in combination with copper(II) salts, AADO undergoes a structural alteration and self-assembles with copper ions leading to the formation of multinuclear complexes (Fig. 1.13a).

K. J. Oliver et al. discovered that when $CuCl_2$ was used as a copper salt, a multinuclear copper complex **17** with the D6R structure was formed (Fig. 1.13b).[27] During complexation, AADO underwent a structural change to pyrazole. Additionally, a reduction in the copper ion from divalent to monovalent was observed. J. Otsuki et al. discovered that when AADO is mixed with $Cu(NO_3)_2$ in water, its active methylene groups undergo nitrosation to form trioxime. Subsequently, self-assembly of these trioxime molecules with copper(II) ions results in the formation of a pentanuclear copper complex **18** (Fig. 1.13c).[28]

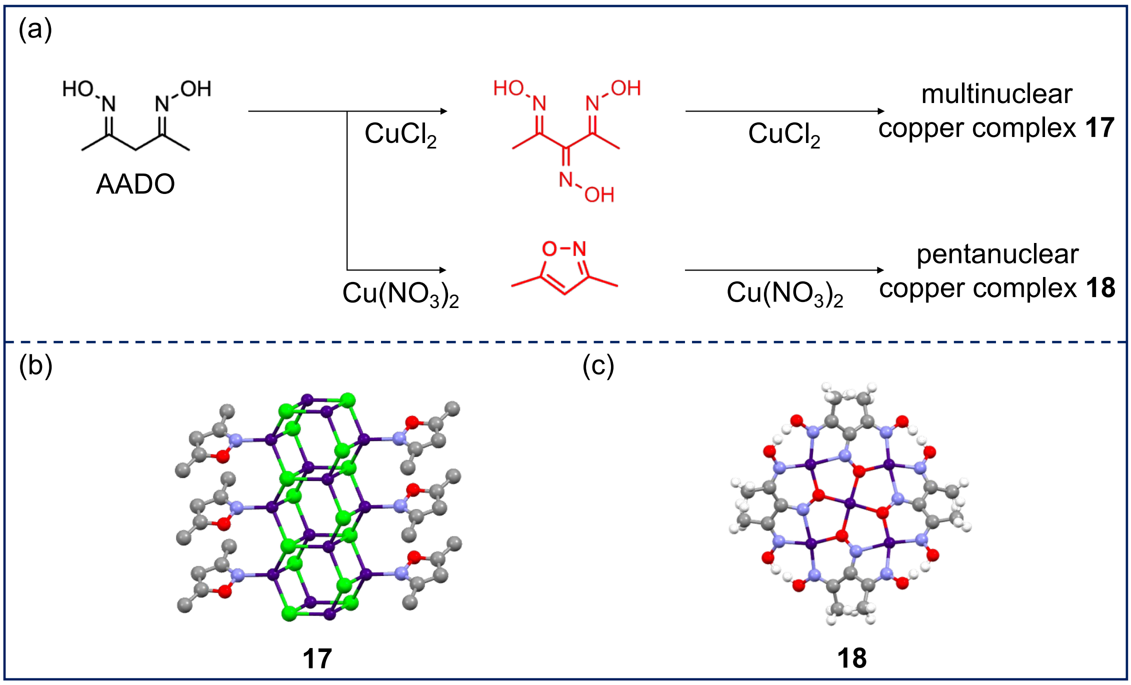

Fig. 1.13. Multinuclear copper complex formation via spontaneous reaction and self-assembly from AADO and copper ions (H, white; C, gray; N, blue; O, red; Cl, green; Cu, purple). (a) Reaction formulae. (b) Crystal structure of complex **17**. (c) Crystal structure of complex **18**.

1-4. Purpose

The objective of this doctoral thesis is to create multinuclear copper complexes through spontaneous reactions and self-assembly, characterize these complexes, and provide guidelines for the facile preparation of functional multinuclear metal complexes.

In Chapter 2, our aim was to generate multinuclear metal complexes using simple organic ligands and metal salts through spontaneous reactions and self-assembly. Multinuclear copper complexes were formed when cyclic 1,3-dione dioxime derivatives were mixed with copper(II) nitrate.

Chapter 3 aimed to demonstrate the functions and properties of multinuclear metal complexes formed via spontaneous reactions and self-assembly. Specifically, the magnetic properties of the obtained multinuclear copper complexes were elucidated.

1-5. References

1. A. Arbaoui, C. Redshaw and D. L. Hughes, *Chem Commun (Camb)*, 2008, DOI: 10.1039/b810417d, 4717-4719.
2. P. K. Saini, C. Romain and C. K. Williams, *Chem Commun (Camb)*, 2014, **50**, 4164-4167.
3. B. D. Nath, K. Takaishi and T. Ema, *Catalysis Science & Technology*, 2020, **10**, 12-34.
4. L.-J. Wu, W. Lee, P. Kumar Ganta, Y.-L. Chang, Y.-C. Chang and H.-Y. Chen, *Coord. Chem. Rev.*, 2023, **475**.
5. B. Gholamkhass, H. Mametsuka, K. Koike, T. Tanabe, M. Furue and O. Ishitani, *Inorg. Chem.*, 2005, **44**, 2326-2336.
6. K. Yamauchi, S. Masaoka and K. Sakai, *J. Am. Chem. Soc.*, 2009, **131**, 8404-8406.
7. H. Takeda and O. Ishitani, *Coord. Chem. Rev.*, 2010, **254**, 346-354.
8. M. Okamura, M. Kondo, R. Kuga, Y. Kurashige, T. Yanai, S. Hayami, V. K. Praneeth, M. Yoshida, K. Yoneda, S. Kawata and S. Masaoka, *Nature*, 2016, **530**, 465-468.
9. M. Yoshizawa, M. Tamura and M. Fujita, *Science (Washington, DC, U. S.)*, 2006, **312**, 251-254.
10. J. S. Miller and A. J. Epstein, *Angewandte Chemie International Edition in English*, 1994, **33**, 385-415.
11. R. Sessoli, H. L. Tsai, A. R. Schake, S. Wang, J. B. Vincent, K. Folting, D. Gatteschi, G. Christou and D. N. Hendrickson, *Journal of the American Chemical Society*, 1993, **115**, 1804-1816.
12. A. B. Gaspar, V. Ksenofontov, M. Seredyuk and P. Gütlich, *Coord. Chem. Rev.*, 2005, **249**, 2661-2676.
13. R. Clérac, H. Miyasaka, M. Yamashita and C. Coulon, *Journal of the American Chemical Society*, 2002, **124**, 12837-12844.
14. M. G. F. Vaz, L. M. M. Pinheiro, H. O. Stumpf, A. F. C. Alcantara, S. Golhen, L. Ouahab, O. Cador, C. Mathoniere and O. Kahn, *Chem. - Eur. J.*, 1999, **5**, 1486-1495.
15. G. A. Craig, G. Velmurugan, C. Wilson, R. Valiente, G. Rajaraman and M. Murrie, *Inorg. Chem.*, 2019, **58**, 13815-13825.
16. Y. Liu, D. Shi and F. Xu, *Polyhedron*, 2022, **226**.
17. B. Kersting, G. Steinfeld and D. Siebert, *Chemistry – A European Journal*, 2001, **7**, 4253-4258.
18. J. Tercero, C. Diaz, J. Ribas, J. Mahia and M. A. Maestro, *Inorg. Chem.*, 2002, **41**, 5373-5381.
19. L. Lecren, O. Roubeau, C. Coulon, Y.-G. Li, X. F. Le Goff, W. Wernsdorfer, H. Miyasaka and R. Clerac, *J. Am. Chem. Soc.*, 2005, **127**, 17353-17363.
20. S. Demeshko, G. Leibeling, S. Dechert and F. Meyer, *Dalton Trans*, 2006, DOI: 10.1039/b517254c, 3458-3465.
21. L. Botana, J. Ruiz, J. M. Seco, A. J. Mota, A. Rodriguez-Dieguez, R. Sillanpaa and E. Colacio, *Dalton Trans*, 2011, **40**, 12462-12471.
22. M. L. Tong, Y. M. Wu, Y. X. Tong, X. M. Chen, H. C. Chang and S. Kitagawa, *Eur. J. Inorg. Chem.*,

2003, **2003**, 2385-2388.
23. L. L. Zheng, J. D. Leng, W. T. Liu, W. X. Zhang, J. X. Lu and M. L. Tong, *Eur. J. Inorg. Chem.*, 2008, **2008**, 4616-4624.
24. D. B. Eni, D. M. Yufanyi, J. H. Nono, C. D. Tabong and M. O. Agwara, *Chemical Papers*, 2020, **74**, 3003-3016.
25. L.-L. Zheng, J.-F. Wang, J. Wang, A.-J. Zhou, C.-X. Liao and S. Hu, *Inorganica Chim. Acta*, 2020, **501**.
26. L.-L. Zheng and S. Hu, *J. Cluster Sci.*, 2022, **33**, 2189-2195.
27. K. J. Oliver, T. N. Waters, D. F. Cook and C. E. F. Rickard, *Inorganica Chim. Acta*, 1977, **24**, 85.
28. J. Otsuki, T. Sekine, Y. Kida, Y. Shinozaki, S. Kobayashi, T. Tamura, K. Sugawa, I. Yoshikawa, H. Houjou, H. Yoshikawa and A. Tsukamoto, *Dalton Trans*, 2017, **46**, 2760-2764.

Chapter 2

Spontaneous Reaction and Self-Assembly of Copper Nitrate and Cyclic 1,3-Dione Dioximes into Multicopper Complexes

2-1. Abstract

We have found that a variety of multinuclear copper complexes are formed via spontaneous reaction and self-assembly under mild conditions simply by mixing cyclic 1,3-dione dioximes and copper(II) nitrate. When cyclohexane-1,3-dione dioxime was employed as the ligand precursor, it led to the formation of a trinuclear copper complex comprising three ligands and three copper(II) ions. All three ligands within the complexes had their active methylene groups oxidized to carbonyl groups. Additionally, two of these ligands underwent further reaction with the solvent MeOH to form a hemiacetal structure. In the crystal structure, the oxime groups coordinated with the copper(II) ions of the neighboring molecule, resulting in the formation of a one-dimensional chain. On the other hand, when cyclopentane-1,3-dione dioxime was utilized as a ligand precursor, the copper(II) ion underwent reduction to a copper(I) ion, forming a dinuclear copper complex comprising three ligands and two copper(I) ions. Two out of the three ligands within the complex were connected by forming a double bond between the active methylene groups. The remaining ligand remained structurally unchanged. These findings suggest that multinuclear metal complexes can be readily formed using simple organic ligands and metal salts through spontaneous reactions and self-assembly.

2-2. Introduction

As shown in Chapter 1, multinuclear metal complexes have attracted attention due to their diverse properties. They are mainly formed from pre-designed ligands and metal ions. In contrast, the formation of multinuclear metal complexes via spontaneous reactions and self-assembly is rare. In 2017, J. Otsuki et al. discovered the formation of a pentanuclear copper complex (Cu_5) through spontaneous reaction and self-assembly from AADO and copper(II) nitrate (Scheme 2.1, top).[1] However, neither the mechanism behind this phenomenon nor its generality was clear, prompting us to investigate whether similar phenomena could be observed by exploring the reactions of several related compounds. In the crystal structure of Cu_5, the ligands derived from AADO adopt a conformation, in which the carbon framework forms a part of a ring structure, with oxime moieties pointing outward. Therefore, we speculated that use of cyclic 1,3-dione dioximes as the ligand precursors would lead to similar structures. Therefore, we used cyclohexane 1,3-dione dioxime, which has a structure where the terminal methyl groups of AADO are joined together with a methylene moiety, and cyclohexane 1,3-dione dioxime, which has a structure where the terminal methyl groups of AADO are joined directly together, as the ligand precursors. However, we found that the combination of these organic molecules with copper(II) nitrate gave new multinuclear structures. Although the structures obtained were diverse, the ligands in the complexes had one thing in common: the active methylene was altered. In this chapter, we report the crystal structures of these reaction/assembly products and also provide some insights into the common mechanisms of the reactions.

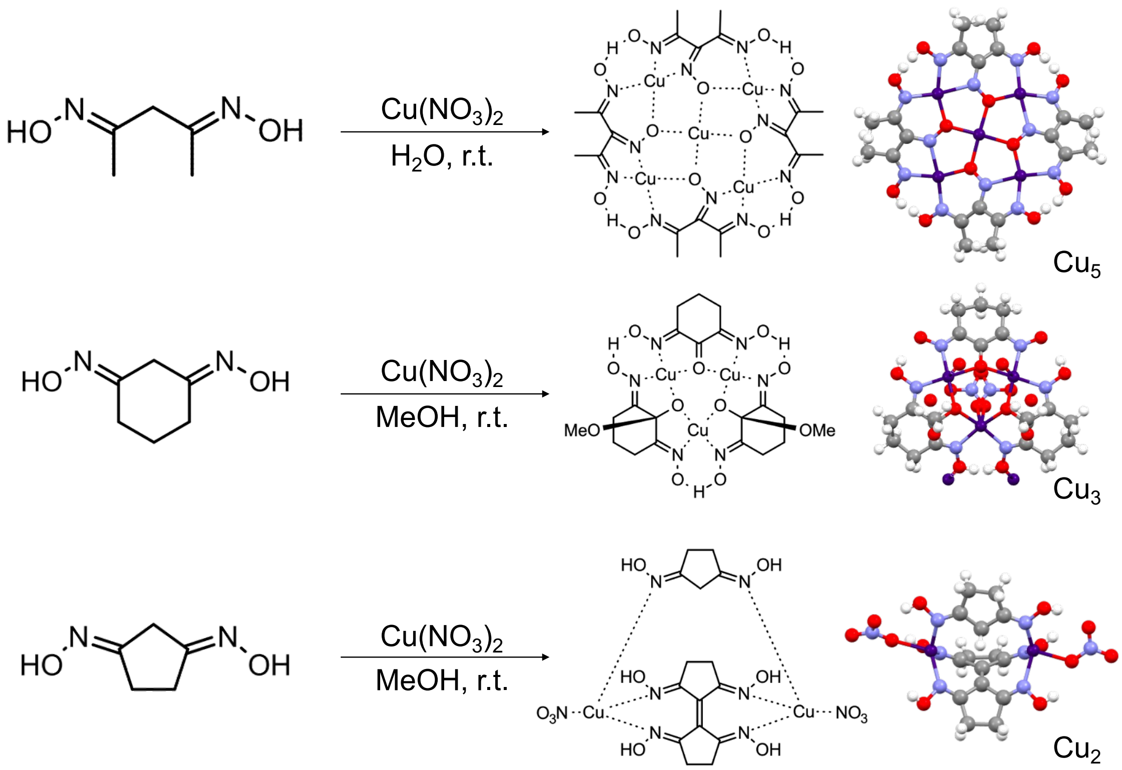

Scheme 2.1. Multinuclear copper complexes formation from 1,3-dione dioximes and copper(II) nitrate via spontaneous reaction and self-assembly.

2-3. Result and Discussion

A methanol solution of cyclohexane-1,3-dioxime and a methanol solution of copper(II) nitrate were mixed and left to stand for 2 weeks at room temperature, allowing the solvent to evaporate slowly, resulting in the precipitation of green plate-like single crystals (yield: 35%). The single crystal X-ray crystallography showed that the crystal composed of a trinuclear copper complex (Cu_3) comprising three ligands and three copper(II) ions, as shown in Fig. 2.1a (space group: *Cm* (No. 8)). The crystallographic data is summarized in Table 2.1. All ligands within the trinuclear copper complex had their active methylene groups oxidized, converting into carbonyl groups. Among the three ligands, two formed hemiacetal structures due to the methanol solvent. This complex exhibits a crystallographic mirror plane passing through C1, O1, and Cu2. Each trinuclear copper complex contains one nitrate ion per molecule as an anion. These nitrate ions are disordered over two equivalent positions related by the mirror plane. Electron density remaining near the nitrate ions was tentatively assigned to water molecules without settled hydrogen atoms.

Cu1 and Cu1' (the prime designates crystallographically equivalent atom) are equivalent, but due to the disorder in the nitrate ions, one forms an octahedral coordination structure while the other forms a square pyramidal coordination structure. Cu1 and Cu1' are coordinated by two oxygen atoms (bond distances of 2.00 Å and 1.94 Å to O1 and O3, respectively) from the active methylene groups of the ligands, and two oxime nitrogen atoms (1.95 Å and 1.94 Å to N1 and N2, respectively), forming an N_2O_2 basal plane. The oxime oxygen atom of the neighboring molecule coordinate at the apical positions (2.38 Å to O5). Cu1 or Cu1' forming the octahedral coordination structure coordinate oxygen atoms of the nitrate ions at the remaining apical positions (2.50 Å to O9). Cu2 adopts a square pyramidal coordination structure, forming an N_2O_2 basal plane similar to those of Cu1 and Cu1', with two nitrogen atoms (1.96 Å to N3 and N3') and two oxygen atoms (1.96 Å to O3 and O3'). Oxygen atoms of the nitrate ions coordinate at the apical positions (2.26 Å to O7).

The alignment of the three ligands is strengthened by hydrogen bonding between the hydrogen atom of the oxime and the deprotonated oxygen atom of the other oxime. The distances O2–O4 (2.57 Å) and O5–O5' (2.48 Å) are considerably shorter than the typical hydrogen bond distance range of 2.7 to 3.0 Å. Specifically, the hydrogen bond with lengths below 2.5 Å fall under the classification of a low-barrier hydrogen bond.[2, 3] To confirm the hydrogen bonding from the crystallography data, the oxime hydrogen atoms involved in these hydrogen bonds were intentionally removed, and electron density was confirmed as depicted in Fig. 2.1b. In the case of O2–O4, the high-density region, as indicated by the arrow, is observed closer to O4 than O2. In contrast, the high-density region is observed right in the middle of O5 and O5', suggesting that the hydrogen is not localized, which aligns with the low-barrier hydrogen bonds. These types of hydrogen bonds were also observed in the previously reported pentanuclear complex Cu_5.[1]

The three copper ions form recurring structure (–Cu–O–Cu–) with the three oxygens from the active methylene groups of the ligands. The oxime oxygens O5 and O5’ coordinate with the copper ions Cu1 and Cu1’ of adjacent complexes in the *c*-axis direction, forming a one-dimensional coordination chain as illustrated in Fig. 2.1c.

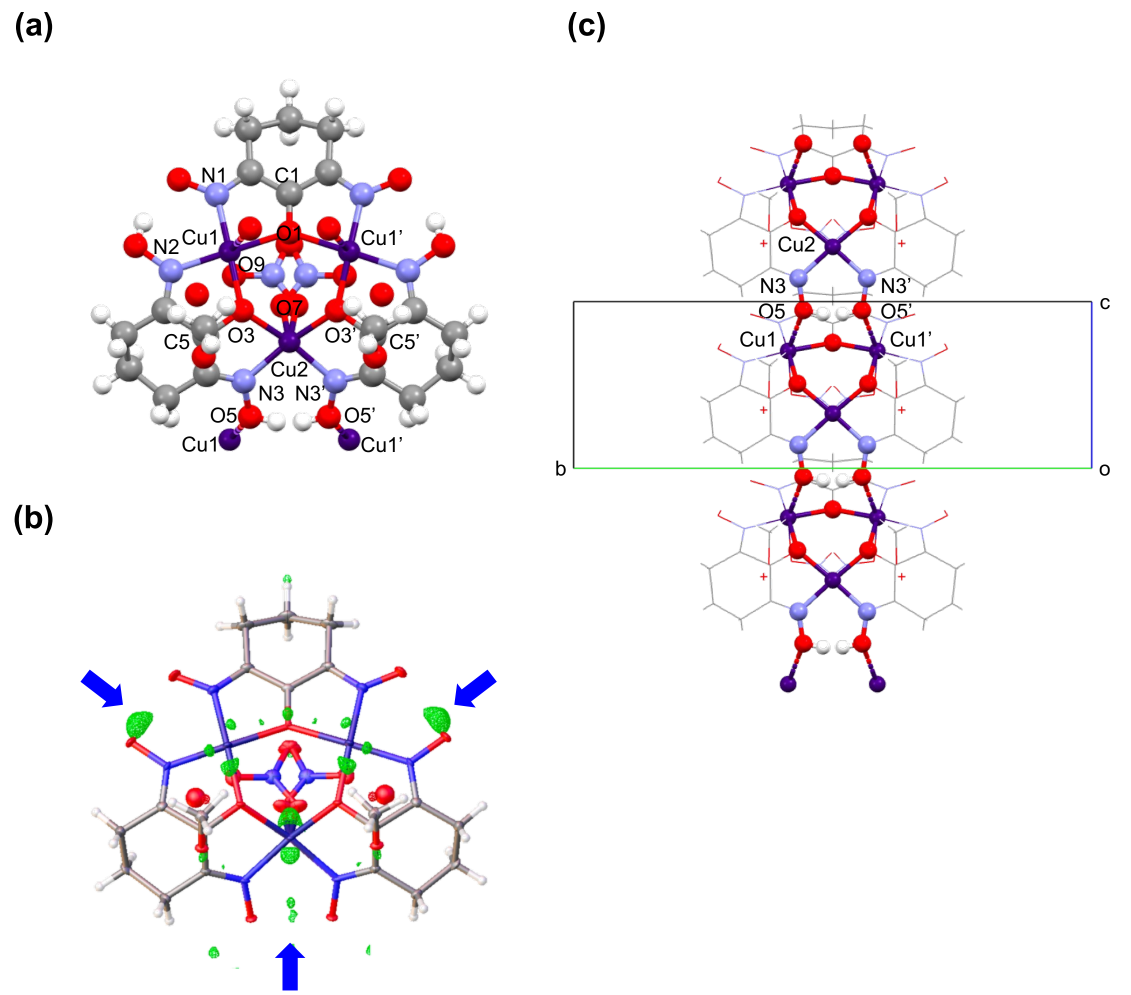

Fig. 2.1. A trinuclear copper complex formed from cyclohexane-1,3-dione dioxime and copper(II) nitrate. (a): Crystal structure of one molecule., (b): The residual electron density map of the hypothetical structure with omitted hydrogen atoms in the oxime moiety. Green: positive; red: negative., (c): One-dimensional chains.

The most notable feature found in the crystals is that the active methylene of 1,3-dione dioxime was oxidized to a carbonyl group. Two of the carbonyl groups reacted with the solvent methanol, turning them into hemiacetals. There is a report of similar reactions observed with 1,3-diones, where oxidation produces ketones or *gem*-diols at the 2-position.[4] Oxidation of active methylene to carbonyl groups by metal ions has also been reported for 1,3-diimine compounds.[5-9]

The finding that the active methylene of 1,3-dione dioxime is oxidized to the carbonyl group under mild conditions in the presence of copper(II) nitrate has important implications for the nitrosation reaction of the active methylene of AADO, which was previously reported by J. Otsuki et al. and whose mechanism has not been clarified. When active methylene is oxidized to a carbonyl group in the presence of copper(II) nitrate (Scheme 2.2i), a disproportionation reaction with unoxidized, unreacted AADO may occur. This leads to the formation of the trioxime (Scheme 2.2ii).

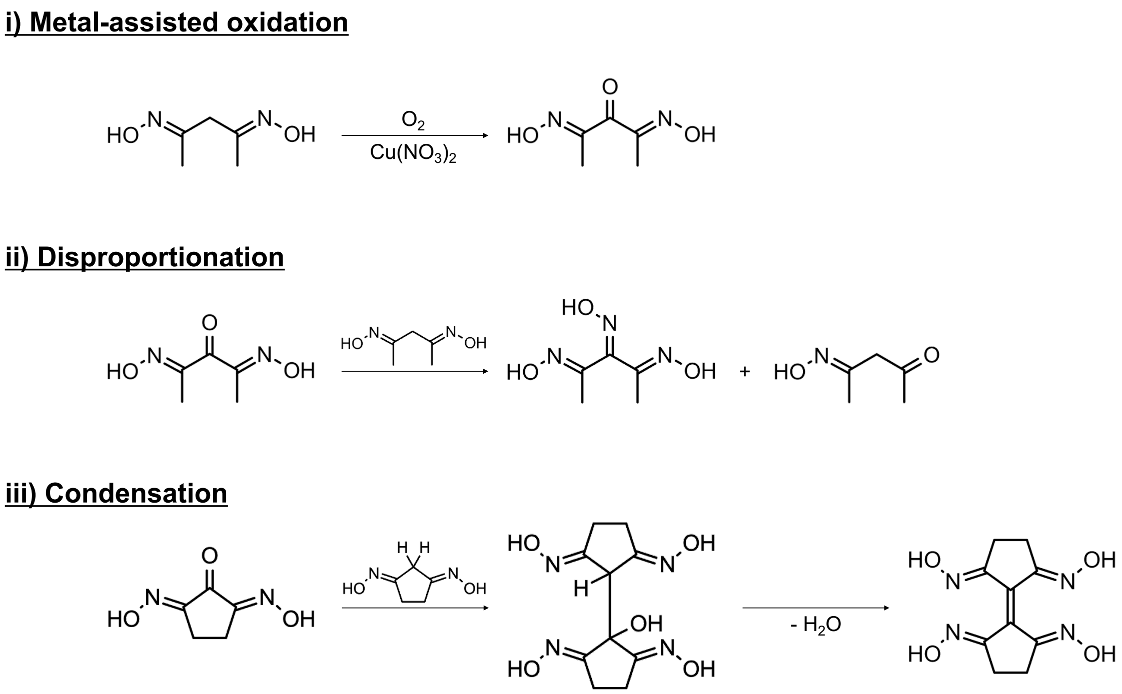

Scheme 2.2. Structural changes of 1,3-dione dioxime in the presence of copper(II) nitrate.

Cyclopentane-1,3-dione dioxime was used as a ligand precursor and mixed with copper(II) nitrate, resulting in another spontaneous reaction and self-assembly in MeOH solution, which was observed to produce a dinuclear copper complex (Cu_2) shown in Fig. 2.2. The crystal data for this complex are summarized in Table 2.1, where the space group of the crystal was $P\bar{1}$ (No. 2). There is void spaces in the crystal lattice, which are presumably occupied by disordered solvent molecules (MeOH). This disordered region could not be modeled by molecular structures and was therefore treated with the solvent mask function of the OLEX2 software.

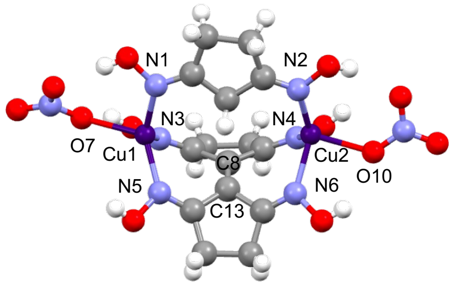

Fig. 2.2. Crystal structure of Cu_2 formed from cyclopentane-1,3-dione dioxime and copper(II) nitrate.

Both copper ions have a tetrahedral coordination structure, which is typical of copper(I) ion.[10-12] The tetrahedral structure is formed with three oxime nitrogen atoms and one oxygen atom from the nitrate ion; the bond lengths for Cu1 and Cu2 are as follows: cyclopentane oxime nitrogen atoms (1.97 Å and 1.95 Å to N1 and N2, respectively), the oxime nitrogen atoms of the cyclopentane dimer (2.00 Å and 2.09 Å to N5 and N3, 2.02 Å and 2.05 Å to N4 and N6, respectively), and nitrate oxygen atoms (2.33 Å and 2.16 Å to O7 and O10, respectively). The positive charges of copper ions are neutralized by two nitrate ions.

The formation of the C=C bond in the active methylene may be explained by the involvement of a carbonyl intermediate, as shown in Scheme 2.2iii. At first, similar to other 1,3-dione dioximes, the active methylene group undergoes oxidation to form a carbonyl group. The nucleophilic attack on the carbonyl carbon by the carbon flanked by the dioxime moieties of the unreacted cyclopentane-1,3-dione dioxime, which is likely in the enamine form, followed by dehydration, results in the formation of the dimer bridged by the double bond. The Aldol-type condensation in 1,3-dione compounds is a known reaction.[13, 14]

2-4. Conclusion

In this chapter, it was found that a multinuclear copper complex is formed simply by mixing cyclic 1,3-dione dioxime with copper(II) nitrate under mild conditions. When cyclohexane-1,3-dione dioxime was used as a ligand precursor, a trinuclear copper complex was formed, consisting of three copper(II) ions and three ligands whose active methylene groups were changed into carbonyl groups, two of which formed hemiacetal with methanol from the solvent. In the crystal, the complex formed a one-dimensional chain with the oxime group also coordinating to the copper(II) ion of the neighboring molecule. When cyclopentane-1,3-dione dioxime was used as a ligand precursor, copper(II) was reduced to copper(I) and two ligand precursors formed a double bond into a dimer. Furthermore, a dinuclear copper complex was formed from the unreacted ligand, the dimer and three copper(I) ions. These results demonstrate the generality of the spontaneous reaction and self-assembly strategy, by which multinuclear copper complexes are formed from 1,3-dione dioxime and copper(II) nitrate.

2-5. Experimental Section

Preparation of Materials and Single Crystals. Cyclohexane-1,3-dione dioxime and cyclopentane-1,3-dione dioxime were prepared from the corresponding diones and hydroxyammonium hydrochloride according to a literature method[15]. A solution of $Cu(NO_3)_2$ (649 mg, 2.68 mmol) in MeOH (1.0 mL) and a solution of cyclohexane-1,3-dione dioxime (568 mg, 4.00 mmol) in MeOH (24 mL) were combined and left standing at room temperature allowing slow evaporation. Green plate crystals, which were deposited after 2 weeks, were collected (245 mg, yield: 35%; Anal. Calcd. for $[Cu_3(C_6H_7N_2O_3)(C_7H_{10}N_2O_4)_2(NO_3)](H_2O)_{0.42}$: C 30.49; H 3.56; N 12.45. Found: C 30.56; H 3.63; N 12.44.). On a solution of $Cu(NO_3)_2$ (35 mg, 0.10 mmol) in MeOH (0.3 mL), pure MeOH and a solution of cyclopentane-1,3-dione dioxime (26 mg, 0.20 mmol) in MeOH (0.75 mL) were successively layered in a vial, which was left standing in a refrigerator. Brown plate crystals, which were deposited after 2 weeks, were collected (11 mg).

Measurements. The single crystal diffraction analysis data were collected with a Rigaku VariMax Dual with a Saturn diffractometer at 93 K (for Cu_3) and with a Rigaku XtaLABminiII at room temperature (for Cu_2), both using Mo Kα radiation (0.71075 Å). The structures were solved by the direct method using SHELXT[16] and refined by the full-matrix least-squares method using SHELXL[17] with the help of graphical user interface supplied by ShelXle[18] and OLEX2[19]. Thermogravimetric analysis was conducted with a Rigaku Thermoplus TG8120 instrument.

2-6. Appendix

The crystal data for Cu_3 and Cu_2 have been deposited with the Cambridge Crystallographic Data Centre as supplementary publications No. CCDC 2104277 and No. CCDC 2104276.

Table 2.1. Crystallographic data.

Compound	Cu_3	Cu_2
Empirical formula	$C_{10}H_{13.91}Cu_{1.5}N_{3.5}O_{7.21}$	$C_{15}H_{20}Cu_2N_8O_{12}$
Moiety formula	$\{[Cu_3(C_6H_7N_2O_3)(C_7H_{10}N_2O_4)_2(NO_3)]\}_{0.5}(H_2O)_{0.21}$	$Cu_2(C_5H_8N_2O_2)(C_5H_6N_2O_2)_2(NO_3)_2$
Formula weight	393.79	631.47
Temperature/K	93 (2)	293 (2)
Crystal system	monoclinic	triclinic
Space group	*Cm* (No.8)	$P\bar{1}$ (No.2)
a/Å	8.7907 (2)	9.5500 (4)
b/Å	21.7758 (6)	11.0660 (5)
c/Å	7.0174 (2)	12.4013 (5)
α/°	90	75.298 (4)
β/°	92.886 (2)	77.731 (3)
γ/°	90	80.393 (3)
Volume/Å^3	1341.60 (6)	1229.83 (9)
Z	4	2
ρ_{calc} g/cm^3	1.950	1.705
μ/mm^{-1}	2.444	1.804
F (000)	798.0	640.0
Crystal size/mm^3	0.2 × 0.2 × 0.01	0.3 × 0.1 × 0.01
Radiation	Mo Kα (λ = 0.71073 Å)	Mo Kα (λ = 0.71073 Å)
2θ range for data collection/°	5.002 to 57.39	3.832 to 52.74
Index ranges	$-11 \leq h \leq 11, -28 \leq k \leq 28, -7 \leq l \leq 9$	$-11 \leq h \leq 11, -13 \leq k \leq 13, -15 \leq l \leq 15$
Reflections collected	6843	18505
Independent reflections	2671 [R_{int} = 0.0644, R_{sigma} = 0.0527]	4977 [R_{int} = 0.0741, R_{sigma} = 0.0892]
Data/restraints/parameters	2671/34/230	4977/0/340
Goodness-of-fit on F^2	0.920	1.032
Final R indexes [$I \geq 2\sigma(I)$]	R_1 = 0.0274, wR_2 = 0.666	R_1 = 0.0709, wR_2 = 0.1513
Final R indexes [all data]	R_1 = 0.0300, wR_2 = 0.0679	R_1 = 0.1178, wR_2 = 0.1707
Largest diff. peak/hole/e Å^{-3}	0.53/-0.41	0.89/-0.47
Flack parameter	0.015 (14)	

2-7. References

1. J. Otsuki, T. Sekine, Y. Kida, Y. Shinozaki, S. Kobayashi, T. Tamura, K. Sugawa, I. Yoshikawa, H. Houjou, H. Yoshikawa and A. Tsukamoto, *Dalton Trans*, 2017, **46**, 2760-2764.
2. V. W. H. Day, Alamgir Md.; Kang, Sung Ok; Powell, Douglas; Lushington, Gerald; Bowman-James, Kristin, *Journal of the American Chemical Society*, 2007, **129**, 8692-8693.
3. C. L. Perrin, *Acc. Chem. Res.*, 2010, **43**, 1550-1557.
4. A. Sivan and A. Deepthi, *Tetrahedron Lett.*, 2014, **55**, 1890-1893.
5. S. Yokota, Y. Tachi and S. Itoh, *Inorg. Chem.*, 2002, **41**, 1342-1344.
6. J. D. Azoulay, R. S. Rojas, A. V. Serrano, H. Ohtaki, G. B. Galland, G. Wu and G. C. Bazan, *Angew. Chem. Int. Ed. Engl.*, 2009, **48**, 1089-1092.
7. M. L. Scheuermann, A. T. Luedtke, S. K. Hanson, U. Fekl, W. Kaminsky and K. I. Goldberg, *Organometallics*, 2013, **32**, 4752-4758.
8. A. Kalita, V. Kumar and B. Mondal, *RSC Advances*, 2015, **5**, 643-649.
9. A. Sokolohorskyj, O. Železník, I. Císařová, J. Lenz, A. Lederer and J. Merna, *J. Polym. Sci., Part A: Polym. Chem.*, 2017, **55**, 2440-2449.
10. B. J. Hathaway, *Coord. Chem. Rev.*, 1981, **35**, 211-252.
11. D. B. Rorabacher, *Chem. Rev.*, 2004, **104**, 651-697.
12. J. P. Sauvage, *Angew. Chem. Int. Ed. Engl.*, 2017, **56**, 11080-11093.
13. T. Linker and U. Linker, *Angew. Chem. Int. Ed.*, 2000, **39**, 902-904.
14. H. Asahara, S. Kawakami, K. Yoshioka, S. Tani, K. Umezu and N. Nishiwaki, *Bull. Chem. Soc. Jpn.*, 2018, **91**, 1715-1723.
15. A. B. Zaitsev, E. Y. Schmidt, A. M. Mikhaleva, A. V. Afonin and I. A. Ushakov, *Chemistry of Heterocyclic Compounds (New York, NY, United States)*, 2005, **41**, 722-729.
16. G. M. Sheldrick, *Acta Crystallogr A Found Adv*, 2015, **71**, 3-8.
17. G. M. Sheldrick, *Acta Crystallogr A*, 2008, **64**, 112-122.
18. C. B. Hubschle, G. M. Sheldrick and B. Dittrich, *J. Appl. Crystallogr.*, 2011, **44**, 1281-1284.
19. O. V. Dolomanov, L. J. Bourhis, R. J. Gildea, J. A. K. Howard and H. Puschmann, *J. Appl. Crystallogr.*, 2009, **42**, 339-341.

Chapter 3

Alterations in Magnetic Properties of Crystals of Trinuclear Copper Complexes: Isolated Entities Versus One-Dimensional Chains

3-1. Abstract

We obtained two crystal structures of trinuclear copper complexes that were nearly identical in structure by altering the recrystallization conditions. In one crystal, the oxime group from the neighboring trinuclear copper complex coordinated with two copper ions within the complex, leading to the formation of a one-dimensional chain. Conversely, in the other crystal, no such chains were formed, and the trinuclear copper complex molecules remained isolated. The distinct molecular arrangements resulted in differing magnetic properties between the two crystals. The crystal forming the one-dimensional chain exhibited weakly ferromagnetic intermolecular interactions, while the crystal lacking these chains showed no intermolecular interactions, leaving the complex molecules magnetically isolated. This approach represents a novel method for easily altering the molecular arrangements of multinuclear metal complexes created through spontaneous reactions and self-assembly. Thereby, allowing for fine-tuning the accompanying magnetic properties.

3-2. Introduction

Chapter 2 explained in detail the formation of multinuclear copper complexes through spontaneous reactions and self-assembly under mild conditions. These reactions occurred when various 1,3-dione dioxime derivatives as simple organic molecules were mixed with copper(II) nitrate as metal salt. Among the obtained compounds, it is anticipated that the trinuclear copper complex will exhibit characteristic magnetic properties derived from its molecular arrangement, forming one-dimensional chains in the crystal. Several examples have been reported where properties are altered by changing the molecular arrangement in crystals.[1-4] In the study of magnetic properties, it has been observed that heating mononuclear copper complexes alters their magnetic behavior.[3, 4] In contrast, some researchers have manipulated the crystalline arrangements of multinuclear complexes using bridging ligands or counterions to modify their magnetic properties.[5-10] However, our study stands apart as we discovered instances where the molecular arrangement of trinuclear copper complexes can be changed solely by selecting specific crystallization conditions, without relying on additional bridging ligands, as will be explained in detail in this Chapter. With specific examples, the new approach showed that the molecular arrangement within crystals of multinuclear metal complexes, created through spontaneous reactions and self-assembly, can be easily modified, leading to changes in associated properties.

3-3. Result and Discussion

Green plate-like single crystals were obtained from a methanol solution containing cyclohexane-1,3-dione dioxime and copper(II) nitrate. The crystals are denoted as $[Cu_3]_{MeOH}$ (Fig. 3.1). As detailed in Chapter 2, in this crystal, the active methylene groups of the three cyclohexane-1,3-dione dioximes were oxidized to carbonyl groups, two of which formed hemiacetals with the solvent methanol and self-assembled with copper(II) ions to form a trinuclear copper complex.[11] Parts of ligands of the complex also coordinated with copper ions of neighboring complexes, forming one-dimensional chains. These crystals were dissolved in H_2O and the pH was adjusted to 10 by adding 2 M NaOH. Slow evaporation of the solvent yielded blue blocky crystals, which are denoted $[Cu_3]_{Aq}$ (yield: 68%; Anal. Calcd. for $[Cu_3(C_6H_8N_2O_4)_3(\mu\text{-}H_2O)(H_2O)](H_2O)_4$: C 26.52; H 4.45; N 10.31. Found: C 26.47; H 4.63; N 10.28.). The homogeneity of both crystals, $[Cu_3]_{MeOH}$ and $[Cu_3]_{Aq}$, was confirmed by the consistency of the powder X-ray diffraction of both samples with the diffraction patterns simulated from the single crystal structures (Fig. 3.2).

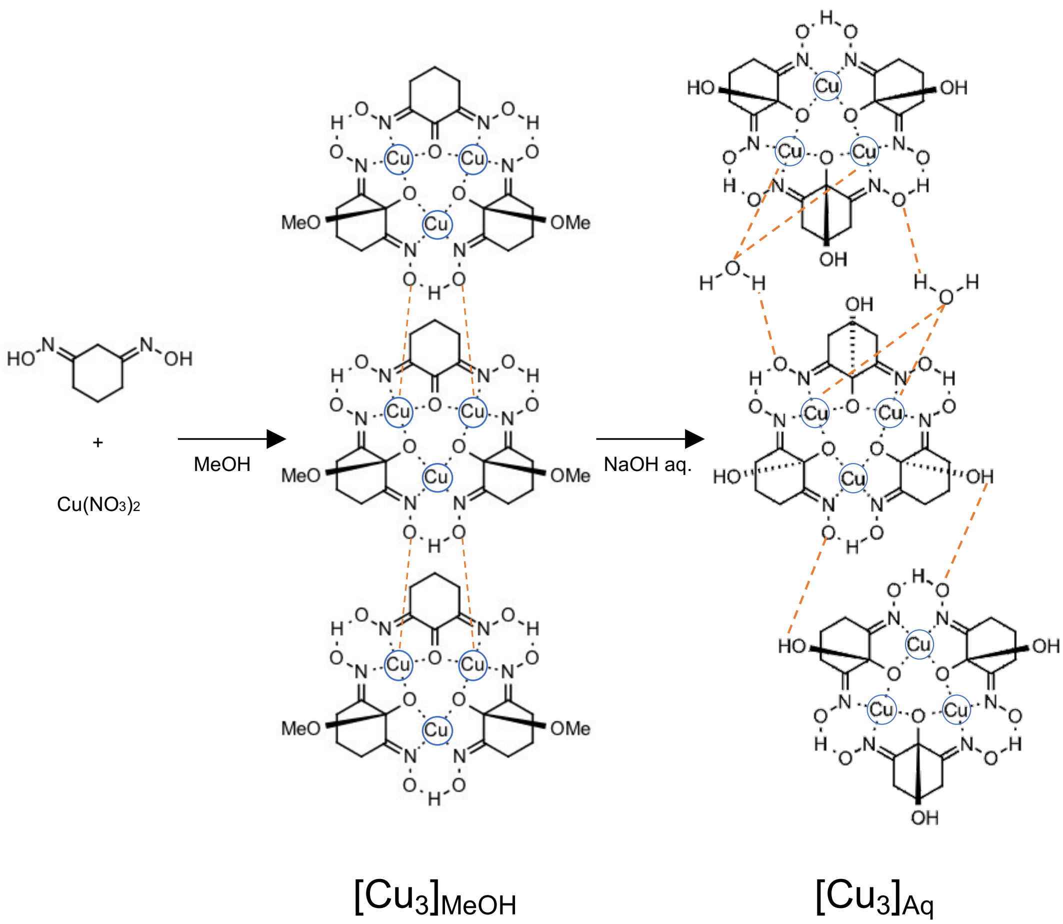

Fig. 3.1. Spontaneous reaction and self-assembly and subsequent rearrangement of complexes in the crystal. The nitrate ions coordinating to copper(II) ions are omitted in $[Cu_3]_{MeOH}$.

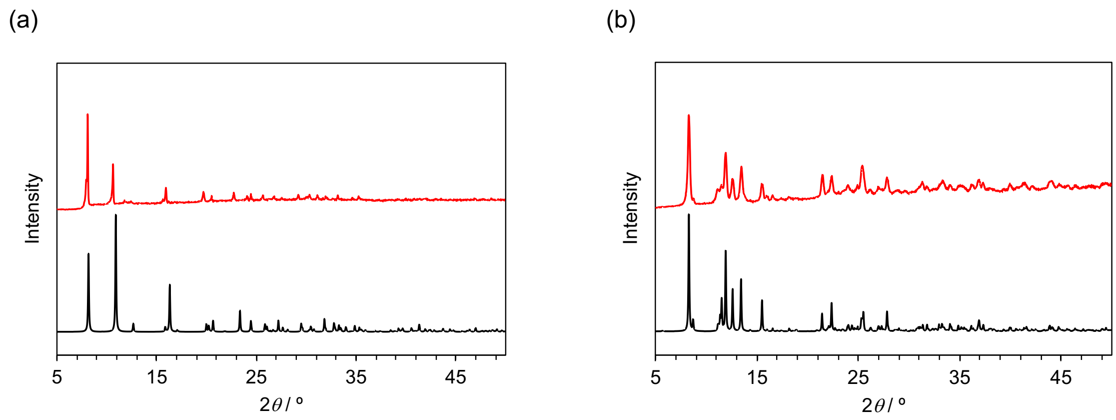

Fig. 3.2. Comparison of powder X-ray patterns (red: observed spectrum for the crystals, black: calculated spectrum from single crystal data): (a) $[Cu_3]_{MeOH}$, (b) $[Cu_3]_{Aq}$.

Although the crystal structure of $[Cu_3]_{MeOH}$ has already been described in detail in Chapter 2, the crystallographic data and structure are reproduced in Table 3.1 and Fig. 3.3a for easy comparison with those of $[Cu_3]_{Aq}$.

Crystallographic data for $[Cu_3]_{Aq}$ has been summarized in Table 3.1, and its structure is depicted in Fig. 3.3c. The overall triangular structure remains consistent with $[Cu_3]_{MeOH}$. However, all three carbonyl groups of the ligands form acetals with the solvent water. All copper ions coordinate with two acetal oxygen atoms and two nitrogen atoms from the oxime groups, forming N_2O_2 basal planes similar to $[Cu_3]_{MeOH}$. Each copper ion coordinates with water at the apex position, adopting a square pyramidal coordination structure. Cu1 and Cu2 are doubly bridged by the oxygen of the same water molecule (μ_2-O16) and the acetal oxygen. On the other hand, both Cu1–Cu3 and Cu2–Cu3 are exclusively bridged by the acetal oxygen. Unlike $[Cu_3]_{MeOH}$, where copper ions form one-dimensional coordination chains, in $[Cu_3]_{Aq}$, there are at least four atoms separating copper ions from adjacent complexes, isolating the copper ions of each complex from those of neighboring complexes. Therefore, simply conducting a recrystallization led to alterations in intermolecular interactions among the complexes. It is anticipated that these changes in intermolecular connectivity could impact the magnetic properties.

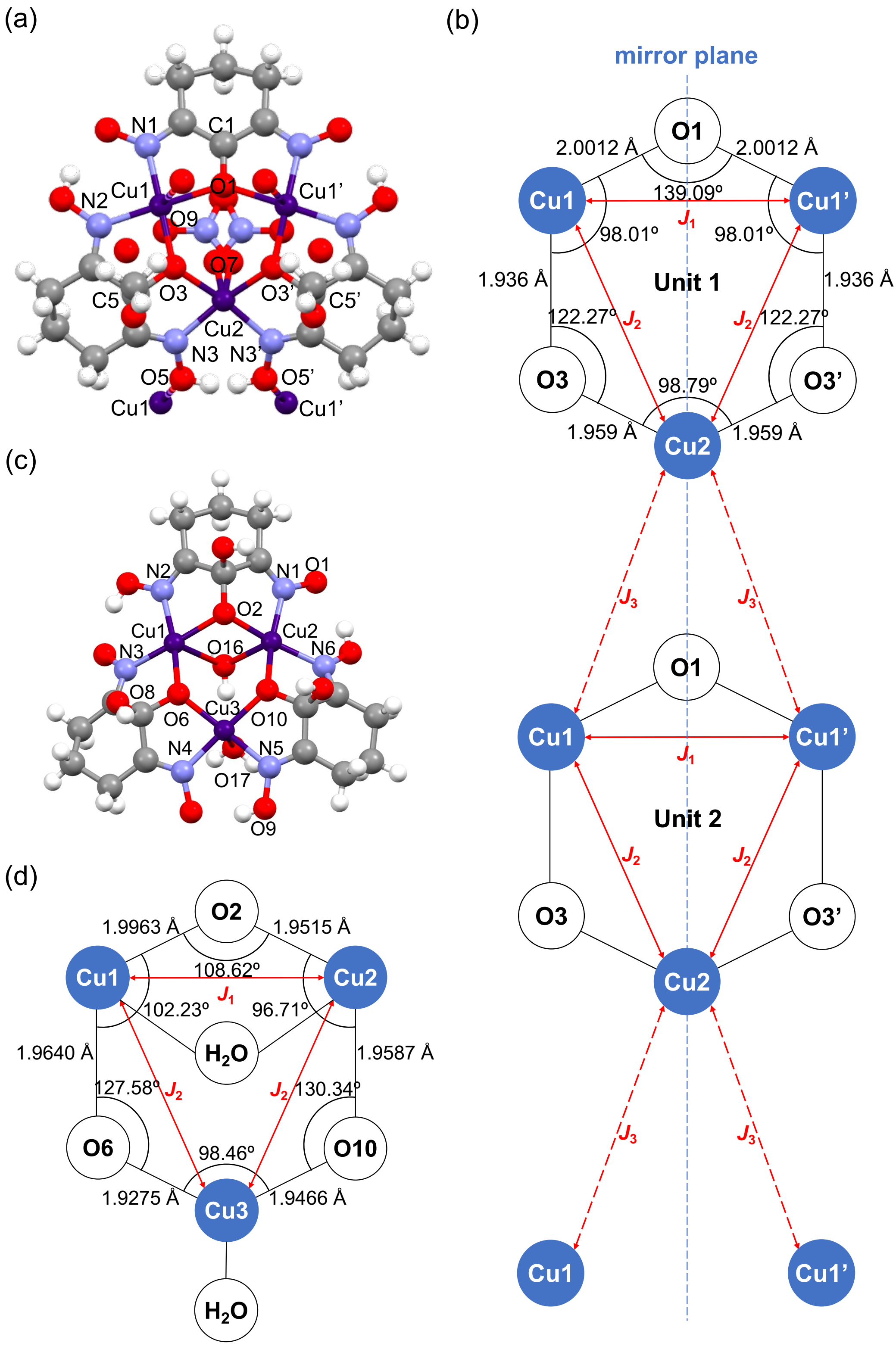

Fig. 3.3. Trinuclear copper complexes. [Cu$_3$]$_{MeOH}$: (a) structure, (b) magnetic interaction model and bond distances and angles. [Cu$_3$]$_{Aq}$: (c) structure, (d) magnetic interaction model and bond distances and angles.

The magnetization of these complexes was examined using SQUID-VSM as a function of magnetic field strength and temperature (2 K to 300 K). As shown in Fig. 3.4, the magnetization of both complexes exhibits a linear dependency on the applied magnetic field at both low and high temperatures. Concerning the temperature dependence of $[Cu_3]_{Aq}$, the $\chi_m T$ value was 1.1 $cm^3\ mol^{-1}\ K$ at 300 K, gradually decreasing with decreasing temperature to a constant value below approximately 60 K, reaching 0.51 $cm^3\ mol^{-1}\ K$ at 2.5 K (Fig. 3.5a). This behavior suggests that the ground state is a doublet, which is dominant at low temperatures and mixed with higher multiplicities at higher temperatures. To quantitatively analyze this behavior, we established the model illustrated in Fig. 3.3d. In this complex, all Cu–O bond lengths (1.93–1.99 Å) and O–Cu–O bond angles (97°–102°) were almost identical. However, the Cu1–O2–Cu2 bond angle (109°) significantly differs from the other two angles (Cu1–O6–Cu3 (128°) and Cu2–O10–Cu3 (130°)). Additionally, the coordination environment of Cu3, with H_2O molecules in apical coordination, differs from those of Cu1 and Cu2, where μ-H_2O molecules act as bridging entities. Based on these structural features, we defined the following exchange constants: J_1 for Cu1–Cu2, J_2 for Cu1–Cu3 and Cu2–Cu3, and derived the spin Hamiltonian 3.1.

$$\widehat{H} = -2J_1(\hat{\boldsymbol{s}}_1 \cdot \hat{\boldsymbol{s}}_2) - 2J_2(\hat{\boldsymbol{s}}_1 \cdot \hat{\boldsymbol{s}}_3 + \hat{\boldsymbol{s}}_2 \cdot \hat{\boldsymbol{s}}_3) \qquad (3.1)$$

The molar magnetic susceptibility, χ_m, can be described using the van Vleck equation (eq. 1.4), and *Es* is derived from Hamiltonian 3.1. The term attributed to temperature-independent paramagnetism, which was found to be negligibly small, has been excluded. From fitting across the entire temperature range, the values for the exchange constants and the *g*-factor were determined as J_1 = -58.5 cm^{-1}, J_2 = -45.0 cm^{-1}, and g = 2.32 (refer to Fig. 3.5a, for multiplicities and eigenvalues, see the appendix). As both J_1 and J_2 are negative, it indicates an antiferromagnetic interaction between the copper ions. Both J_1 and J_2 values obtained for these complexes were of the same order as those reported for multinuclear copper complexes where two copper ions are bridged by a single oxygen atom.[12, 13]

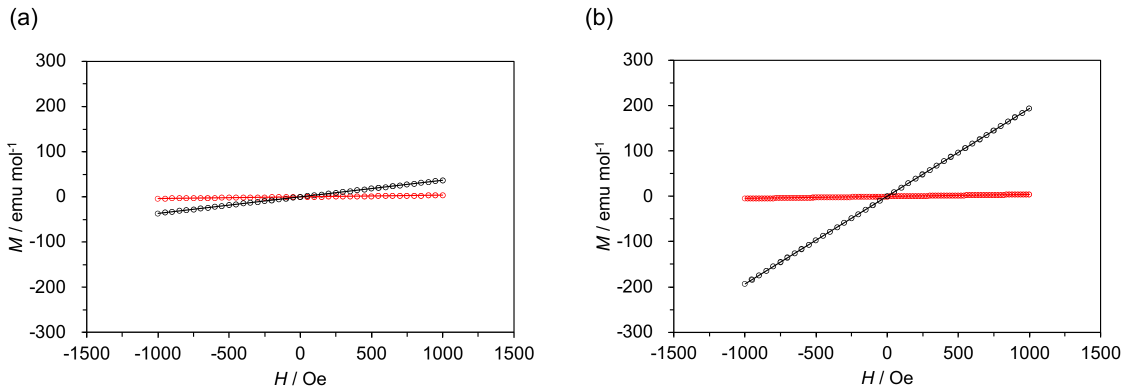

Fig. 3.4. The magnetic field dependence of magnetization (circles: observed values; lines: fitted lines): (a) $[Cu_3]_{MeOH}$ at 2 K (black) and 300 K (red), (b) $[Cu_3]_{Aq}$ at 2.6 K (black) and 300 K (red).

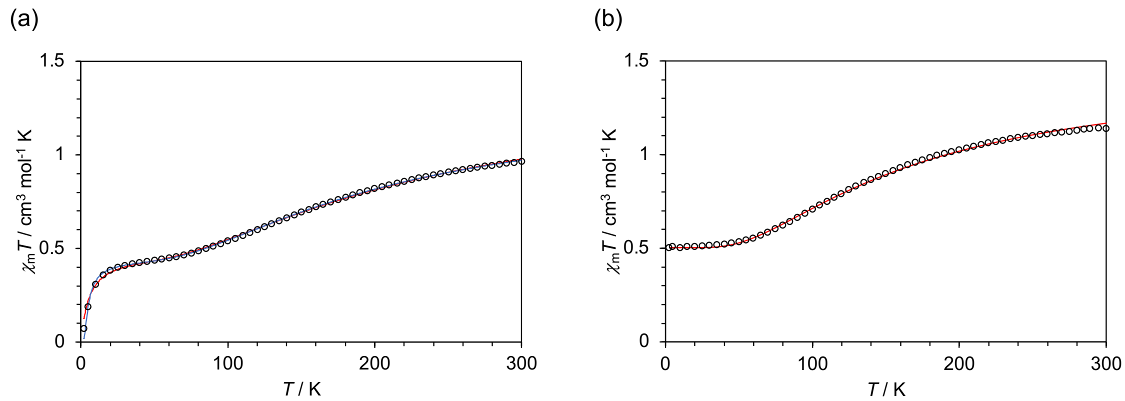

Fig. 3.5. Molar magnetic susceptibilities measured from 300 K to 2 K (practically the same results were obtained when temperature was raised from 2 K to 300 K). Black open circles indicate observed values. (a) $[Cu_3]_{Aq}$. Red line represents the simulated results. (b) $[Cu_3]_{MeOH}$. Red and blue lines represent the simulated results using the mean-field approximation and the dimer model with a periodic boundary condition, respectively.

For $[Cu_3]_{MeOH}$, a similar trend to $[Cu_3]_{Aq}$ was observed where the $\chi_m T$ gradually decreased as the temperature was lowered from 300 K to around 60 K and the decrease became more gradual below the temperature range. However, the magnetization sharply approached zero below 20 K (Fig. 3.5b). The decrease to zero magnetization at low temperatures suggests the existence of weak intermolecular interactions that cancel out the magnetic moment of the trinuclear complexes. To quantitatively describe this magnetic behavior, a model was created considering the structural features illustrated in Fig. 3.3b. While Cu1 and Cu1' are crystallographically equivalent, Cu2 has different coordination geometries (139° for Cu1–O–Cu1' and 122° for Cu1 (Cu1')–O-Cu2) and coordinating atoms. While Cu1 (Cu1') coordinates with carbonyl and hemiacetal oxygen, Cu2 coordinates with two hemiacetal oxygens. Based on this structural features, the exchange constants are defined as: J_1 for Cu1–Cu1' and J_2 for Cu1–Cu2 and Cu1'–Cu2. Additionally, this complex forms a one-dimensional chain, and the Cu1 (Cu1') and Cu2 of neighboring complexes are bridged by two oxime groups (N–O). Consequently, intermolecular magnetic interactions might be mediated. One approach to model this situation is through the mean-field approximation.[9] The molar magnetic susceptibility χ including the mean-field exchange interaction zJ_{ex} is expressed in eq 3.2.

$$\chi T = \frac{\chi_m T}{1 - \frac{2zJ_{ex}}{N_A \mu_0 \mu_B{}^2 g^2} \chi_m} \qquad (3.2)$$

Here, χ_m represents the virtual molar magnetic susceptibility of isolated complexes derived from eq 1.4 and 3.1. Applying eq 3.2 to the magnetization data, the values obtained are J_1 = -54.4 cm^{-1}, J_2 = -69.4 cm^{-1}, g = 2.26 and zJ_{ex} = -7.8 cm^{-1} (Fig. 3.5b). The intramolecular J_1 and J_2 are of the same order as $[Cu_3]_{Aq}$. The small value of zJ_{ex} indicates weak intermolecular interactions. The negative values suggest that this interaction is antiferromagnetic when considering the trinuclear complex as one magnetic moment unit.

In an alternative analysis, a two-molecule model of trinuclear copper complexes with a periodic boundary condition, as depicted in Fig. 3.3b, was established. Intermolecular exchange interactions J_3 were introduced for Cu1–N3–O5–Cu2 and Cu'–N3'–O5'–Cu2. The spin Hamiltonian is represented by eq 3.3.

$$\begin{aligned}\hat{H} = &-2J_1 \hat{\boldsymbol{s}}_{1,1} \cdot \hat{\boldsymbol{s}}_{1,1'} - 2J_2(\hat{\boldsymbol{s}}_{1,1} \cdot \hat{\boldsymbol{s}}_{1,2} + \hat{\boldsymbol{s}}_{1,1'} \cdot \hat{\boldsymbol{s}}_{1,2}) - 2J_3(\hat{\boldsymbol{s}}_{1,2} \cdot \hat{\boldsymbol{s}}_{2,1} + \hat{\boldsymbol{s}}_{1,2} \cdot \hat{\boldsymbol{s}}_{2,1'}) \\ &-2J_1 \hat{\boldsymbol{s}}_{2,1} \cdot \hat{\boldsymbol{s}}_{2,1'} - 2J_2(\hat{\boldsymbol{s}}_{2,1} \cdot \hat{\boldsymbol{s}}_{2,2} + \hat{\boldsymbol{s}}_{2,1'} \cdot \hat{\boldsymbol{s}}_{2,2}) - 2J_3(\hat{\boldsymbol{s}}_{2,2} \cdot \hat{\boldsymbol{s}}_{1,1} + \hat{\boldsymbol{s}}_{2,2} \cdot \hat{\boldsymbol{s}}_{1,1'}) \qquad (3.3)\end{aligned}$$

The first and second subscripts on $\hat{s}$ denote the complexes (Unit 1, Unit 2) and the copper ions, respectively. The final term represents the periodic boundary condition. Fitting across the entire temperature range yielded values of J_1 = -24.5 cm^{-1}, J_2 = -77.2 cm^{-1}, J_3 = 3.69 cm^{-1} and g = 2.18 (Fig. 3.5b). The positive value of J_3 indicates ferromagnetic intermolecular copper-copper interactions between the complexes. As mentioned earlier, the trinuclear copper complex forms a one-dimensional coordination chain in $[Cu_3]_{MeOH}$. The copper ions between complexes in this crystal are bridged by the oxime group. The nitrogen atom on the Cu2 side is part of the basal plane and coordinates with the $d_{x^2-y^2}$ spin orbital, while the oxygen atom on the Cu1 (Cu1') side is at the apex, coordinating with the non-spin d_{z^2} orbital. Therefore, interactions between these copper ions are expected to be small.[14] The small estimated value of 3.69 cm^{-1} aligns with this expectation. With $|J_1|$ smaller than $|J_2|$, the spins of Cu1 and Cu1' align more parallel to each other in the ground state, while the spin of Cu2 is antiparallel to them. In this circumstance, the ferromagnetic interaction of Cu2 with Cu1 and Cu1' from neighboring complexes causes the spin orientation within the complex to alternate along the one-dimensional chain, leading to an overall cancellation of magnetization within the crystal. The *g*-values of both crystals closely match those obtained from the ESR spectra (Fig. 3.6). While the reason for the relatively high *g*-value for $[Cu_3]_{Aq}$ remains unclear, such *g*-values are not unprecedented in the literature.[6, 15]

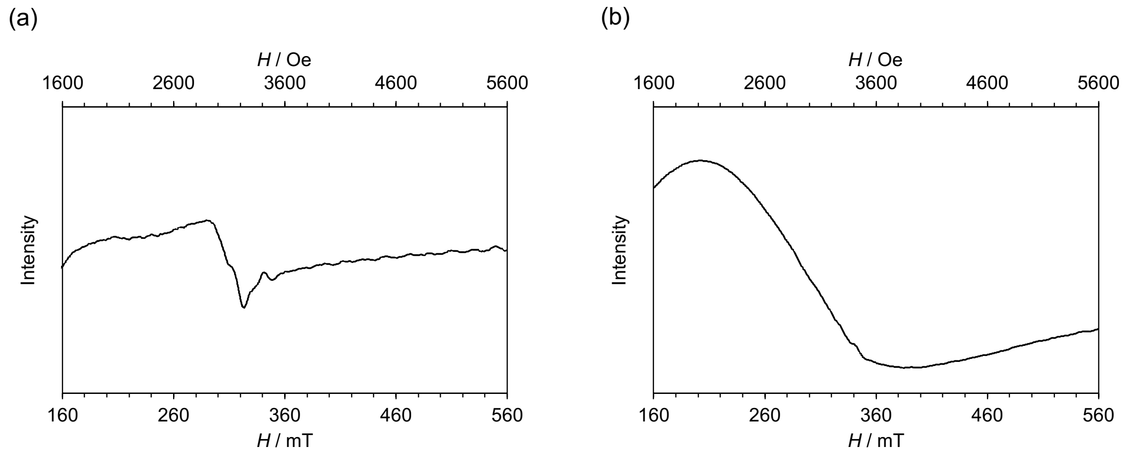

Fig. 3.6. The X-band ESR spectra of trinuclear copper complexes: (a) $[Cu_3]_{MeOH}$, (b) $[Cu_3]_{Aq}$.

3-4. Conclusion

In this chapter, we were able to elucidate changes in magnetic properties by altering the molecular arrangement of trinuclear copper complexes. We discovered that even without the addition of a bridging ligand, trinuclear copper complexes with nearly identical molecular structures exhibit different molecular arrangements in different crystalline states depending on the recrystallization conditions. In one crystal, the spin interactions behaved as isolated complexes, while in the other crystal, the spin interactions occurred between the complexes and were observed to form one-dimensional chains. This study experimentally demonstrated that the molecular arrangement of multinuclear metal complexes, created by spontaneous reactions and self-assembly, can be easily altered, leading to corresponding changes in their properties.

3-5. Experimental Section

Recrystallization from a basic aqueous solution. The trinuclear copper complex was prepared from cyclohexane-1,3-dione dioxime and copper(II) nitrate in methanol according to a literature method.[11] The pH of a solution of this trinuclear copper complex (17 mg, 0.022 mmol) in H_2O (20 mL) was adjusted to 10 by the addition of 2 M NaOH (20 mL) and the solution was left standing at room temperature allowing slow evaporation. Blue block crystals, which were deposited after 5 days, were collected (12 mg, 68%).

Measurements. The single crystal diffraction analysis data were collected with a Rigaku XtaLAB mini II diffractometer at room temperature using the Mo Kα radiation (0.71075 Å). The structures were solved by the direct method using SHELXT[16] and refined by the full-matrix least-squares method using SHELXL[17] with the help of graphical user interface supplied by Olex2.[18] Characterization of magnetization was carried out on a Quantum Design MPMS3 SQUID magnetometer with the VSM mode (sensitivity: 1×10^{-8} emu). Several milligrams of the crystals wrapped in aluminium foil was used as a sample. The contribution of the aluminium foil to magnetization was subtracted by measuring the foil alone under the same conditions. The X-band ESR measurements were performed on a JEOL JES-RE2X Electron Spin Resonance Spectrometer at room temperature. Microwave powers were set to 60 mW for $[Cu_3]_{MeOH}$ and 30 mW for $[Cu_3]_{Aq}$ and the microwave frequency was 9.2 GHz. Powder X-ray diffraction was measured on a PANalytical X'Pert PRO MPD diffractometer in a reflection mode.

3-6. Appendix

3-6-1. Crystal Structure Information

The crystal data for $[Cu_3]_{Aq}$ has been deposited with the Cambridge Crystallographic Data Centre as supplementary publication No. CCDC 2302585.

Table 3.1. Crystallographic data of trinuclear copper complexes.

Compound	$[Cu_3]_{MeOH}$[11]	$[Cu_3]_{Aq}$
Empirical formula	$C_{10}H_{13.91}Cu_{1.5}N_{3.5}O_{7.21}$	$C_{18}H_{36}Cu_3N_6O_{18}$
Moiety formula	$\{[Cu_3(C_6H_7N_2O_3)(C_7H_{10}N_2O_4)_2(NO_3)]\}_{0.5}(H_2O)_{0.21}$	$[Cu_3(C_6H_8N_2O_4)_3(H_2O)(H_2O)](H_2O)_4$
Formula weight	393.79	815.15
Temperature/K	93 (2)	298.15
Crystal system	monoclinic	triclinic
Space group	*Cm* (No.8)	$P\bar{1}$ (No.2)
a/Å	8.7907 (2)	8.3541 (2)
b/Å	21.7758 (6)	11.4631 (2)
c/Å	7.0174 (2)	16.7008 (4)
α/°	90	100.913 (2)
β/°	92.886 (2)	104.433 (2)
γ/°	90	104.362 (2)
Volume/Å^3	1341.60 (6)	1445.69 (6)
Z	4	2
ρ_{calc} g/cm^3	1.950	1.873
μ/mm^{-1}	2.444	2.279
F (000)	798.0	834.0
Crystal size/mm^3	0.2 × 0.2 × 0.01	0.4 × 0.2 × 0.1
Radiation	Mo Kα (λ = 0.71073 Å)	Mo Kα (λ = 0.71073 Å)
2θ range for data collection/°	5.002 to 57.39	5.126 to 61.404
Index ranges	$-11 \leq h \leq 11, -28 \leq k \leq 28, -7 \leq l \leq 9$	$-11 \leq h \leq 11, -16 \leq k \leq 16, -23 \leq l \leq 23$
Reflections collected	6843	28375
Independent reflections	2671 [R_{int} = 0.0644, R_{sigma} = 0.0527]	8454 [R_{int} = 0.0448, R_{sigma} = 0.0449]
Data/restraints/parameters	2671/34/230	8454/0/435
Goodness-of-fit on F^2	0.920	1.088
Final R indexes [$I \geq 2\sigma(I)$]	R_1 = 0.0274, wR_2 = 0.666	R_1 = 0.0395, wR_2 = 0.1016
Final R indexes [all data]	R_1 = 0.0300, wR_2 = 0.0679	R_1 = 0.0562, wR_2 = 0.1094
Largest diff. peak/hole/e Å^{-3}	0.53/-0.41	1.45/-1.02
Flack parameter	0.015 (14)	

Table 3.2. Bond lengths and angles.

Category	$[Cu_3]_{MeOH}$[11]		$[Cu_3]_{Aq}$	
bond lengths for basal atoms / Å	Cu1–N1	1.949(4)	Cu1–N2	1.955(2)
	Cu1–N2	1.942(3)	Cu1–N3	1.947(2)
	Cu1–O1	2.0012(13)	Cu1–O2	1.9963(16)
	Cu1–O3	1.936(3)	Cu1–O6	1.9640(16)
	Cu2–N3	1.962(3)	Cu1–O16	2.491(2)
	Cu2–O3	1.959(3)	Cu2–N1	1.9518(19)
			Cu2–N6	1.962(2)
			Cu2–O2	1.9515(16)
			Cu2–O10	1.9587(16)
			Cu2–O16	2.347(2)
			Cu3–N4	1.943(2)
			Cu3–N5	1.947(2)
			Cu3–O6	1.9275(16)
			Cu3–O10	1.9466(16)
bond lengths for apical atoms / Å	Cu1–O5	2.374(3)	Cu1–O16	2.491
	Cu1–O9	2.497(7)	Cu2–O16	2.347(2)
	Cu2–O7	2.264(6)	Cu3–O17	2.544
bond angles / °	N1–Cu1–N2	96.42(15)	N2–Cu1–N3	94.98(9)
	N1–Cu1–O1	81.71(16)	N2–Cu1–O2	81.50(8)
	N2–Cu1–O3	82.94(13)	N3–Cu1–O6	81.65(8)
	O1–Cu1–O3	98.01(13)	O2–Cu1–O6	102.23(7)
	N3–Cu2–N3’	94.4(2)	N1–Cu2–N6	95.38(8)
	N3–Cu2–O3	82.17(13)	N1–Cu2–O2	84.07(7)
	O3–Cu2–O3’	98.79(17)	N6–Cu2–O10	81.49(7)
			O2–Cu2–O10	96.71(7)
			N4–Cu3–N5	95.15(8)
			N4–Cu3–O6	83.45(8)
			N5–Cu3–O10	83.03(7)
			O6–Cu3–O10	98.46(7)
	Cu1–O1–Cu1’	139.09(19)	Cu1–O2–Cu2	108.62(8)
	Cu1–O3–Cu2	122.27(14)	Cu1–O16–Cu2	82.96(7)
			Cu1–O6–Cu3	127.58(8)
			Cu2–O10–Cu3	130.34(9)

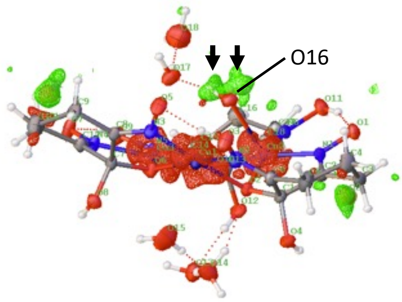

Fig. 3.7. The residual electron densities for $[Cu_3]_{Aq}$. The hydrogen atoms from $H_2O(16)$ has been deliberately removed. The electron densities pointed by the pair of arrows strongly suggest that the species containing O16 is not a OH ion but a H_2O molecule.

3-6-2. Bond Valence Sum Analysis

The bond valence sum analysis was carried out for 5 Cu atoms using the formula.[19, 20]

The oxidation state V of a metal which are coordinated by donor atoms is given by summing up the contribution of every atom i.

$$V = \sum_i \exp\left(\frac{R_0 - R_i}{B}\right) \qquad (3.4)$$

where R_i is the distance between the donor atom and the metal, R_0 is a constant determined for a particular combination of a metal oxidation state and a donor atom, and B is a constant, for which a value of 0.37 is commonly used. The R_0 values were taken from the latest list obtained from "https://www.iucr.org/resources/data/datasets/bond-valence-parameters." The top values were used from the multiple parameter values given for the same a metal oxidation state and a donor atom. The results shown in Table 3.3 clearly demonstrate that every bond valence sum value is most consistent with the Cu(II) oxidation state.

Table 3.3. Bond valence sum analysis.

		Cu(I)	Cu(II)	Cu(III)
$[Cu_3]_{MeOH}$	Cu1	1.51	2.36	2.62
	Cu2	1.38	2.07	2.28
$[Cu_3]_{Aq}$	Cu1	1.45	2.16	2.39
	Cu2	1.54	2.26	2.50
	Cu3	1.54	2.28	2.52

3-6-3. Eigenvalues of Spin Hamiltonians

[Cu3]Aq

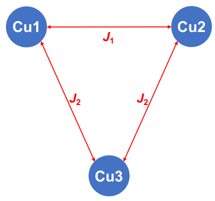

The Hamiltonian is given by eq 3.1

The three-spin system consists of $2^3 = 8$ states in total, which are 1 quartet (*S* = 3/2) and 2 (*S* = 1/2) doublets. The eigenvalues (as functions of J_1 and J_2) and eigenstates were obtained by diagonalizing the Hamiltonian matrix with regard to the uncoupled microstates using a Mathematica code. The results are as follows.

S	E_S
3/2	$-\frac{1}{2}J_1 - J_2$
1/2	$-\frac{1}{2}J_1 + 2J_2$
1/2	$\frac{3}{2}J_1$

[Cu3]MeOH

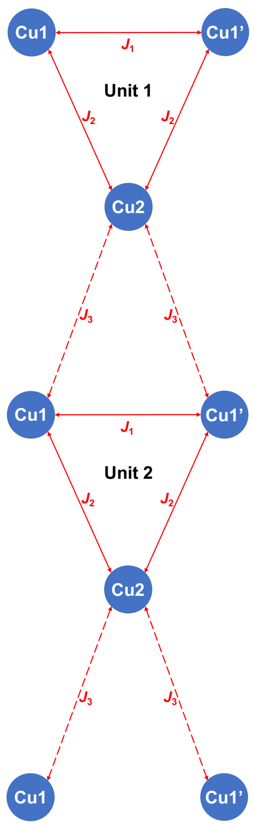

To account for the intermolecular interaction, two trinuclear complexes are juxtaposed and intermolecular interaction J_3 and a periodic boundary condition are introduced. Accordingly, the Hamiltonian is given by eq 3.3.

There are $2^6 = 64$ states, which consist of 1 septet, 5 quartets, 9 triplets, and 5 singlets. The Hamiltonian matrix was diagonalized block-wise for each M_S values (coupled magnetic quantum numbers; M_S = 3, 2, 1, 0 separately to obtain eigenvalues as functions of J_1, J_2, and J_3. The matrix sizes are $1 \times 1, 6 \times 6, 15 \times 15, 20 \times 20$ for M_S = 3, 2, 1, 0, respectively. The results in the Mathematica notation are as follows (j1, j2, j3 should read J_1, J_2, J_3, respectively. Root[formula(#1) &, *k*] (*k* = 1,2,3) indicates the *n*-th solution to the equation formula(#1) = 0 where #1 is the variable.

S = 3 (1 state)

-j1 - 2 j2 - 2 j3

S = 2 (5 states)

j1 - j2 - j3 (doubly degenerate)

-j1 + j2 + j3

1/2 (-2 j1 - j2 - j3 - Sqrt[9 j2^2 - 14 j2 j3 + 9 j3^2])

1/2 (-2 j1 - j2 - j3 + Sqrt[9 j2^2 - 14 j2 j3 + 9 j3^2])

S = 1 (9 states)

3 j1

-j1 + j2 + j3

1/2 (2 j1 + j2 + j3 - Sqrt[9 j2^2 - 14 j2 j3 + 9 j3^2]) (doubly degenerate)

1/2 (2 j1 + j2 + j3 + Sqrt[9 j2^2 - 14 j2 j3 + 9 j3^2]) (doubly degenerate)

Root[j1^3 - 3 j1^2 j2 - 6 j1 j2^2 + 8 j2^3 - 3 j1^2 j3 + 12 j1 j2 j3 - 8 j2^2 j3 - 6 j1 j3^2 - 8 j2 j3^2 + 8 j3^3 + (3 j1^2 - 6 j1 j2 - 6 j2^2 - 6 j1 j3 + 12 j2 j3 - 6 j3^2) #1 + (3 j1 - 3 j2 - 3 j3) #1^2 + #1^3 &, 1]

Root[j1^3 - 3 j1^2 j2 - 6 j1 j2^2 + 8 j2^3 - 3 j1^2 j3 + 12 j1 j2 j3 - 8 j2^2 j3 - 6 j1 j3^2 - 8 j2 j3^2 + 8 j3^3 + (3 j1^2 - 6 j1 j2 - 6 j2^2 - 6 j1 j3 + 12 j2 j3 - 6 j3^2) #1 + (3 j1 - 3 j2 - 3 j3) #1^2 + #1^3 &, 2]

Root[j1^3 - 3 j1^2 j2 - 6 j1 j2^2 + 8 j2^3 - 3 j1^2 j3 + 12 j1 j2 j3 - 8 j2^2 j3 - 6 j1 j3^2 - 8 j2 j3^2 + 8 j3^3 + (3 j1^2 - 6 j1 j2 - 6 j2^2 - 6 j1 j3 + 12 j2 j3 - 6 j3^2) #1 + (3 j1 - 3 j2 - 3 j3) #1^2 + #1^3 &, 3]

S = 0 (5 states)

3 j1,

j1 + 2 j2 + 2 j3 (doubly degenarate)

-j1 + j2 + j3 - Sqrt[9 j2^2 - 14 j2 j3 + 9 j3^2]

-j1 + j2 + j3 + Sqrt[9 j2^2 - 14 j2 j3 + 9 j3^2]

3-7. References

1. M. Kato, *Bull. Chem. Soc. Jpn.*, 2007, **80**, 287-294.
2. H. Ito, M. Muromoto, S. Kurenuma, S. Ishizaka, N. Kitamura, H. Sato and T. Seki, *Nat Commun*, 2013, **4**, 2009.
3. L. Salmon, G. Molnár, S. Cobo, P. Oulié, M. Etienne, T. Mahfoud, P. Demont, A. Eguchi, H. Watanabe, K. Tanaka and A. Bousseksou, *New J. Chem.*, 2009, **33**.
4. A. Benchohra, Y. Li, L. M. Chamoreau, B. Baptiste, E. Elkaim, N. Guillou, D. Kreher and R. Lescouezec, *Angew. Chem. Int. Ed. Engl.*, 2021, **60**, 8803-8807.
5. B. Kersting, G. Steinfeld and D. Siebert, *Chemistry – A European Journal*, 2001, **7**, 4253-4258.
6. J. Tercero, C. Diaz, J. Ribas, J. Mahia and M. A. Maestro, *Inorg. Chem.*, 2002, **41**, 5373-5381.
7. L. Lecren, O. Roubeau, C. Coulon, Y.-G. Li, X. F. Le Goff, W. Wernsdorfer, H. Miyasaka and R. Clerac, *J. Am. Chem. Soc.*, 2005, **127**, 17353-17363.
8. S. Demeshko, G. Leibeling, S. Dechert and F. Meyer, *Dalton Trans*, 2006, DOI: 10.1039/b517254c, 3458-3465.
9. L. Botana, J. Ruiz, J. M. Seco, A. J. Mota, A. Rodriguez-Dieguez, R. Sillanpaa and E. Colacio, *Dalton Trans*, 2011, **40**, 12462-12471.
10. T. R. G. Simoes, M. V. Marinho, J. Pasan, H. O. Stumpf, N. Moliner, F. Lloret and M. Julve, *Dalton Trans*, 2019, **48**, 10260-10274.
11. Y. Hosoya, S. Kobori, Y. Kojima, K. Sugawa and J. Otsuki, *J. Indian Chem. Soc.*, 2021, **98**.
12. G. S. Papaefstathiou, C. P. Raptopoulou, A. Tsohos, A. Terzis, E. G. Bakalbassis and S. P. Perlepes, *Inorg. Chem.*, 2000, **39**, 4658-4662.
13. C. H. Chiang, Y. W. Tzeng, C. I. Yang, M. Nakano, W. L. Wan, L. L. Lai and G. H. Lee, *Dalton Trans*, 2017, **46**, 1237-1248.
14. L. Martínez, C. Bazzicalupi, A. Bianchi, F. Lloret, R. González, C. Kremer and R. Chiozzone, *Polyhedron*, 2017, **138**, 125-132.
15. K. Savithri, B. C. V. Kumar, H. K. Vivek and H. D. Revanasiddappa, *International Journal of Spectroscopy*, 2018, **2018**, 1-15.
16. G. M. Sheldrick, *Acta Crystallogr A Found Adv*, 2015, **71**, 3-8.
17. G. M. Sheldrick, *Acta Crystallogr A*, 2008, **64**, 112-122.
18. O. V. Dolomanov, L. J. Bourhis, R. J. Gildea, J. A. K. Howard and H. Puschmann, *J. Appl. Crystallogr.*, 2009, **42**, 339-341.
19. I. D. Brown, *Acta Crystallographica Section B*, 1992, **48**, 553-572.
20. G. P. Shields, P. R. Raithby, F. H. Allen and W. D. Motherwell, *Acta Crystallogr B*, 2000, **56 (Pt 3)**, 455-465.

Chapter 4

Conclusions and Outlook

4. Conclusions and outlook

Chapter 2 revealed that multinuclear copper complexes formed by simply mixing cyclic 1,3-dione dioxime and copper(II) nitrate. This demonstrates the potential to easily prepare multinuclear metal complexes by gently mixing simple organic ligands and metal ions under mild conditions.

In Chapter 3, the elucidation of the magnetic properties of trinuclear copper complexes derived from cyclohexane-1,3-dione dioxime and copper(II) nitrate demonstrated the potential for easily obtained multinuclear metal complexes to possess magnetic properties. Additionally, by modifying the recrystallization conditions, similar molecular structures but significantly different molecular arrangements were obtained from the original trinuclear copper complex. These complexes displayed differences in magnetic properties due to the disparity in molecular arrangements, indicating the potential to easily alter the structure and properties of obtained complex crystals.

In conclusion, this work provides guidance on the facile preparation of multinuclear metal complexes with complex structures, diverse characteristics, and functionalities by simply mixing simple structured ligands with various metal ions.

Among the multinuclear copper complexes obtained in this work, preliminary results suggested that the trinuclear copper complex formed using cyclohexane-1,3-dione dioxime might function as an electrochemical reduction catalyst in water. Moreover, for other multinuclear copper complexes, changing the recrystallization solvents could alter the molecular arrangements within the crystals, potentially displaying new functionalities and properties.

The finding of several such examples suggests that the formation of multinuclear complexes via spontaneous reactions and self-assembly is likely a common occurrence. This implies that not only copper ions, but metal ions in general, and not limited to 1,3-dione dioximes, but also other organic molecules, might exhibit spontaneous reactivity and self-assembly properties. This methodology holds the potential for broad utilization as a straightforward technique to generate multinuclear metal complexes with novel and intricate structures by simply combining basic organic ligands with diverse metal ions. Additionally, the resulting complexes may demonstrate diverse functions and properties, which are potentially further adjustable by modifying the conditions of recrystallization.

Chapter 5

Acknowledgements

5. Acknowledgements

Part of this work was supported by Kakenhi (18K05156) from the JSPS, Japan and Advanced Research Infrastructure for Materials and Nanotechnology in Japan (ARIM) (23UT-0220) of the MEXT, Japan.

Throughout my work in the laboratory, I received tremendous support from Professor Joe Otsuki, Professor Kosuke Sugawa, Assistant Toshiyuki Ito, and everyone in the Supramolecular Chemistry Lab. Additionally, I am grateful for the invaluable assistance rendered by Professor Arata Tsukamoto and Assistant Professor Hiroki Yoshikawa during the magnetization measurements.